5th INTERNATIONAL MAAR CONFERENCE

Contrasting eruptive styles of late Pleistocene-to-Holocene monogenetic volcanism from maars to domes in the Serdán-Oriental basin, eastern Mexican Volcanic Belt

Post-meeting field guide for the
5th International Maar Conference, Querétaro, México

Gerardo Carrasco-Núñez[1], Michael H. Ort[2], Nancy R. Riggs[2], Brian Zimmer[3], Lorena De León-Barragán[1], Mario López-Rojas[1]

[1] Centro de Geociencias, Universidad Nacional autónoma de México, UNAM Campus Juriquilla, Querétaro, Qro., 76100 México.
[2] Northern Arizona University, Flagstaff, AZ, USA.
[3] Appalachian State University, Boone, NC, USA.

November 23-25, 2014

http://maar2014.geociencias.unam.mx

Cover description: Cerro Pinto, photograph showing unconformable bedding planes at the hinge of the northern tuff ring.
Photo by: Gerardo Carrasco-Núñez.

Universidad Nacional Autónoma de México
Centro de Geociencias

Querétaro, Mexico
November 2014

Edition and design:
J. Jesús Silva Corona

Contrasting eruptive styles of late Pleistocene-to-Holocene monogenetic volcanism from maars to domes in the Serdán-Oriental basin, eastern Mexican Volcanic Belt

Gerardo Carrasco-Núñez[1,*], Michael H. Ort[2], Nancy R. Riggs[2], Brian Zimmer[3], Lorena De León-Barragán[1], Mario López-Rojas[1]

[1] *Centro de Geociencias, Universidad Nacional autónoma de México, UNAM Campus Juriquilla, Querétaro, Qro., 76100 México.*
[2] *Northern Arizona University, Flagstaff, AZ, USA.*
[3] *Appalachian State University, Boone, NC, USA.*
* *gerardoc@geociencias.unam.mx*

INTRODUCTION

The purpose of this field guide is to describe a three-day itinerary to examine examples of recent (late Pleistocene and Holocene) monogenetic volcanism in the eastern Trans-Mexican Volcanic Belt (TMVB; Figure 1) with particular emphasis on the phreatomagmatic structures (maar-type volcanoes). In this area, these include spectacular exposures of deposits from a diversity of eruptive styles and contrasting compositions. The young age of some of these volcanoes and the evolution of some others may be relevant for volcanic hazard assessments within the area. We have selected the most outstanding volcanoes that have easy access for this field trip.

In this field trip, we will focus on maar volcanoes, which in Mexico are collectively named *xalapazcos*, a Nahuatl term meaning "vessel with sand", whereas those craters with an interior lake are called *axalapazcos*. We will have the opportunity to compare different landforms and eruptive products derived from both basaltic and rhyolitic magmas, producing basaltic maar volcanoes *sensu stricto* (where the volcano excavated down into the country rock) such as Atexcac or Aljojuca craters, or Tecuitlapa where a notably well-developed migration of the eruptive locus is observed, a rhyolitic tuff-ring like Tepexitl or a rhyolitic tuff ring-dome complex such as Cerro Pinto, and a large basaltic maar evolving from a strombolian scoria cone at Alchichica.

We will also visit a vitrophyric rhyolite dome (Cerro Pizarro) and Holocene lava flows derived from Los Humeros caldera whose implications for hazard assessment will be discussed. The locations of the volcanoes are shown in Figure 1.

On Day 1, after a 4-hour drive to the Serdán-Oriental Basin, we will explore avalanche-related deposits and explosive products associated with the activity of the Cerro Pizarro rhyolitic dome and discuss the polygenetic origin of what was previously regarded as an isolated monogenetic rhyolitic dome. After that, we will visit rim-caldera basaltic lavas derived from Los Humeros complex and we will pass the Cantona archaeological site, which is regarded as one of the largest pre-Hispanic cities in Mexico.

On Day 2, we will drive to the middle part of the Serdán-Oriental basin to explore different types of volcanoes, starting with Alchichica basaltic crater where we will see the transition from strombolian to phreatomagmatic activity. Then we will explore Cerro Pinto tuff-ring-dome complex volcano, looking at evidence of alternating periods of explosive and effusive activity that produced a complex stratigraphy. After that, we will examine the internal structure of the basaltic Atexcac maar volcano, which records strong interactions with the country rock and vent migration. At the final stop of the day, we will examine pyroclastic sequences of the Tepexitl rhyolitic tuff-ring.

On day 3, we will visit Tecuitlapa and Aljojuca basaltic maars, where we will discuss the influence of the regional tectonic stress regime on the formation of aligned maar and cinder cones and the consequent migration of the eruptive loci following these structural systems, as well as how apparent local hydrologic conditions (Toba café aquifer) favor the formation of dry or wet volcanoes.

REGIONAL GEOLOGIC SETTING

The Serdán-Oriental Basin (SOB) and the Cofre de Perote-Citlaltépetl volcanic range comprises the Eastern Mexican Volcanic Belt (EMVB). This province is characterized by Neogene to Holocene E-W-trending volcanism that goes from the Pacific coast to the Gulf of Mexico covering a large area of Central Mexico (Figure 1). Typical aligned large stratovolcanoes form N-S high volcanic ranges that are cut by large intramontane lacustrine basins such as the SOB in the EMVB. Also, large monogenetic fields including thousands of scoria and lava cones and maar volcanoes, large caldera volcanoes, several rhyolite dome volcanoes, and large silicic calderas form important volumes of recent volcanism. Composition of the magmas is dominantly calc-alkaline, ranging from basalt to rhyolite.

The SOB is dominated by monogenetic bimodal volcanism of Quaternary age, with a minor proportion of isolated Pliocene volcanoes (Negendank *et al.* 1985). Basement Cretaceous limestone rocks and Tertiary intrusive rocks are also exposed in the area (Yáñez and García, 1980), and abundant Miocene volcanic rocks are exposed to the west of the basin (Carrasco-Núñez *et al.*, 1997).

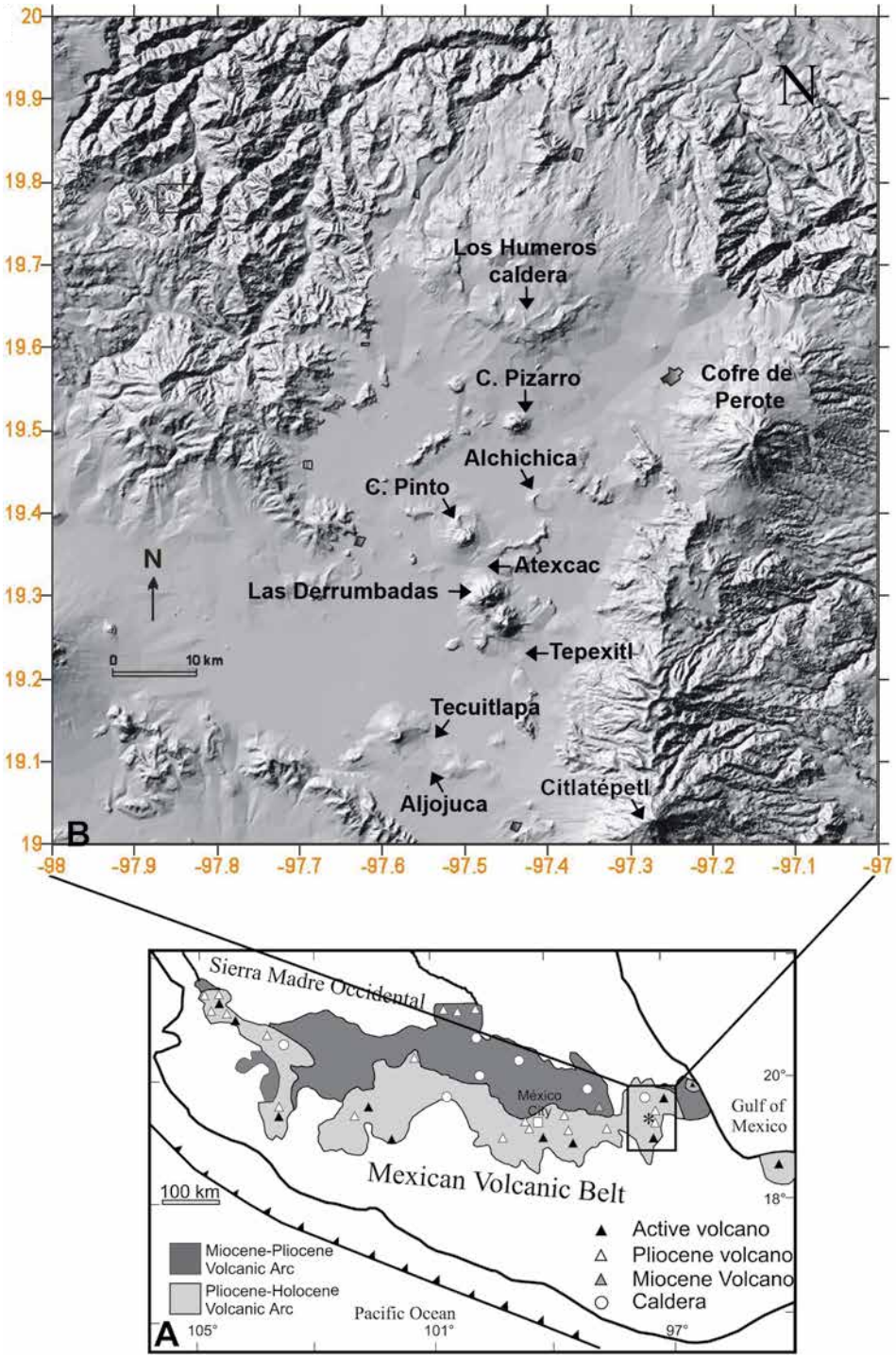

Figure 1. Location of the field trip area in the eastern Trans-Mexican Volcanic Belt (A), and Digital Elevation Model (B) showing the morphology and distribution of the main volcanoes to be explored in the field trip, including Los Humeros caldera, Cerro Pizarro rhyolitic dome, Alchichica crater, Cerro Pinto tuff ring-dome complex, Atexcac maar, Tepexitl tuff-ring, Aljojuca maar and Tecuitlapa maar.

Basement and intrusive rocks

Highly deformed Cretaceous limestone and shale form the regional basement of the EMVB. Palaeozoic crystalline basement are exposed in the Teziutlán massif, northeast of Los Humeros volcano (Viniegra, 1965). These basement rocks are covered by the younger volcanism of the EMVB, but thicken to the north, forming the Sierra Madre Oriental province, a large NW–trending folded and faulted mountain range. Isolated small Oligocene and Miocene plutons of granodiorite, monzonite and syenite intrude the basement rocks (Yáñez and García, 1982). The oldest exposed volcanic rocks in the SOB are andesitic la-

vas of Pliocene age (3.5 Ma, Yañez and García, 1982); however, voluminous Miocene andesitic rocks form the western range of the SOB (Carrasco-Nuñez *et al.*, 1997; Gómez-Tuena and Carrasco-Núñez, 2000).

Serdán-Oriental Basin

The SOB is characterized by monogenetic bimodal (basaltic andesite and rhyolite) volcanism represented by isolated cinder and lava cones of basaltic composition, scattered rhyolitic domes and maar volcanoes, tuff rings and tuff cones. The basin is a broad, internally drained high plain (2,300 m a.s.l.), bounded to the north by the ~20 km-diameter Los Humeros caldera, which has been active since ~0.46 Ma. Voluminous caldera-forming eruptions produced widely distributed pyroclastic ignimbrites and fall deposits that cover the northern part of the Serdán-Oriental basin. The western part of the SOB forms a volcanic range comprising the Miocene andesitic Cerro Grande volcano and the Pleistocene andesitic-dacitic La Malinche stratovolcano, while the eastern edge is formed by the Citlaltépetl-Cofre de Perote range (Figure 1), comprising mainly Quaternary andesitic stratovolcanoes where Citlaltépetl volcano remains active with passive fumarolic activity.

The SOB includes more than 10 maar volcanoes, located in the middle and south portions of the basin. The maars range in composition from basalt to rhyolite, most of them have circular crater shapes, but some others are elliptical and irregular, and some contain a crater lake. There are regional descriptions of these volcanoes (Ordoñez, 1905, 1906; Gasca-Durán, 1981; Siebe *et al.*, 1995) and some have also individually described, such as the multiple-vent Cerro Xalapazco tuff cone (Abrams and Siebe, 1994), Atexcac basaltic maar (Carrasco-Núñez *et al.*, 2007), Cerro Pinto dome-tuff-ring complex (Zimmer *et al.*, 2011), Tepexitl rhyolitic tuff ring (Austin-Erickson, 2007; Austin-Erickson *et al.*, 2011), and Tecuitlapa maar (Ort and Carrasco-Núñez, 2009). Some other maar-volcanoes, such as Alchichica or Aljojuca, are being investigated in detail in current investigations. Most of the cinder cones are isolated in the SOB, although some of them are aligned in E-W or ENE-WSW orientations, particularly in the south, a pattern that is parallel to that shown in the Michoacán-Guanajuato monogenetic field in the central Mexican Volcanic Belt.

Cofre de Perote-Citlaltépetl volcanic range

The Cofre de Perote-Citlaltépetl volcanic range comprises large composite volcanoes of dominantly andesitic-dacitic composition, including the shield-like compound Cofre de Perote (Carrasco-Núñez *et al.*, 2010), La Gloria and Las Cumbres complexes (Rodríguez, 2005) and the currently dormant Citlaltépetl (also called Pico de Orizaba) stratovolcano (Carrasco-Núñez, 2000) (Figure 1). This range represents an important physiographic divide separating the Altiplano (Serdán-Oriental basin) to the west from the Gulf Coastal Plain to the east, with a difference in relief of about 1 km, which in addition with the sloping substrate to the east promoted unstable conditions of the large volcanic edifices forming that range and repeated flank collapses toward the Gulf Coastal Plain (Carrasco-Núñez *et al.*, 2006).

Although Citlaltépetl (Pico de Orizaba) stratovolcano is regarded as the only active volcano within the eastern Trans-Mexican Volcanic Belt, other volcanic activity have occurred in Holocene times such as the pre-Columbian eruption of El Volcancillo at the northern flanks of Cofre de Perote (Siebert and Carrasco-Núñez, 2002) and the recent reports of caldera-rim lavas from Los Humeros volcanic complex (Dávila-Harris and Carrasco-Núñez, 2014) and Aljojuca crater (De León and Carrasco-Núñez, 2014).

VOLCANISM OF THE SERDÁN-ORIENTAL BASIN

Los Humeros Caldera

Los Humeros volcano is one of the largest calderas in central Mexico and hosts one of the most important geothermal fields in the country, producing about 45 MW of power. The evolution of Los Humeros volcano involves the formation of two nested calderas (Los Humeros and Los Potreros) associated with two major silicic ignimbrite-forming eruptions and several plinian eruptions, in addition to dacitic and rhyodacitic dome-forming eruptions and, most recently, central and ring-fracture volcanism dominated by trachydacitic subplinian eruptions intercalated with basaltic and basaltic-andesite lava flows and minor strombolian activity (Ferriz and Mahood, 1984; Willcox, 2011; Dávila-Harris and Carrasco-Núñez, 2014). The first stage started at ~460 ka with a 115 km^3 (DRE) explosive eruption that formed the Los Humeros caldera (21 km x 15 km) and emplaced the widely distributed high-silica rhyolite Xáltipan ignimbrite. Between ~360 ka and 140 ka high-silica rhyolite domes were emplaced, followed by repetitive high silica plinian and sub-plinian eruptions that produced the >10 km^3 (DRE) Faby Formation (Ferriz and Mahood, 1984; Willcox, 2011). A third stage (60-100 ka) started with the eruption of the 15 km^3 (DRE) rhyodacitic and andesitic Zaragoza ignimbrite (Carrasco and Branney, 2005; Carrasco *et al.*, 2012) producing the 9-km-diameter Los Potreros caldera. The Zaragoza ignimbrite exhibits a vertical double compositional zonation (initially rhyodacitic that grades to andesitic and finally return to rhyodacitic again) (Carrasco-Núñez and Branney, 2005) and more recent work suggests that the Zaragoza magma chamber comprises distinct rhyodacite and andesitic components, which apparently form spatially separated

melt lenses as part of a single partly crystallized subvolcanic pluton (Carrasco-Núñez *et al.*, 2012). Several plinian eruptions occurred from >65 to 30 ka (Willcox, 2011), including the formation of the 1.7 km-diameter El Xalapazco crater. Recent studies in the area reveal that the most recent volcanic activity is Holocene and corresponds to the contemporaneous explosive eruption of both rhyodacitic and andesitic tephra of the Cuicuiltic Member, which is younger that 7 ka (Dávila-Harris and Carrasco-Núñez, 2014). The apparently rhythmic alternation of magmas of contrasting composition reveals complex processes in which magmas mingle and mix as part of a heterogeneous and irregular magma chamber with melt zones that are activated by reactivation of surficial faults. The felsic magmas erupted episodically from a central vent area while the basaltic-andesite products were erupted from laterally independent satellite vents located at the eastern part of the caldera as revealed from stratigraphic and isopach and isopleth maps (Dávila-Harris and Carrasco-Nuñez, 2014). The features within these units suggest the existence of separate vents acting simultaneously, while for some other units mingling and efficient mixture of magma is recorded within the juvenile material. Finally, the effusion of ~0.25 km^3 of basaltic andesite and olivine basalt lava flows from the southern margin of Los Humeros caldera occurred in times where the first human settlements were built in the Serdán-Oriental Basin (Figure 2).

Cerro Pizarro rhyolitic dome

Cerro Pizarro rhyolitic dome is a relatively small (2-km-wide, ~700-m-high; ~1.1 km^3), isolated volcano. The volcano is distinctively shaped with a low, broad apron surrounding a resistant ring and a central conical dome. Deep incision is common on the outer flanks of the ring although the west side is open in a horseshoe shape characteristic of collapse volcanoes. Cerro Pizarro has a complex eruptive history including long periods of quiescence and chemical variations that are very uncommon to rhyolite domes (Figure 3a). This complex evolution led Riggs and Carrasco-Núñez (2004) to consider Cerro Pizarro a polygenetic volcano. $^{40}Ar/^{39}Ar$ dates presented by Carrasco-Núñez and Riggs (2008) provide a time frame for this activity.

The evolution of Cerro Pizarro was marked by four main eruptive and erosional stages (Figure 3b). The first stage emplaced deposits considered to represent vent clearing; the oldest are breccias with xenoliths of basement basaltic scoria, Cretaceous limestone, and Xáltipan ignimbrite. Pyroclastic deposits are common, and passive dome emplacement was accompanied by development of a vitrophyric carapace. The early dome collapsed several times around ~220 ka during its growth and block-and-ash-flow deposits are part of the succession.

A second stage at ~ 180 ka emplaced a cryptodome that inflated the volcano and strongly deformed the vi-

Figura 2. Photograph of the Cantona archeological site, built over the Holocene basaltic lava flows from the caldera rim activity of Los Humeros caldera. This site will be visited on Stop A2.2.

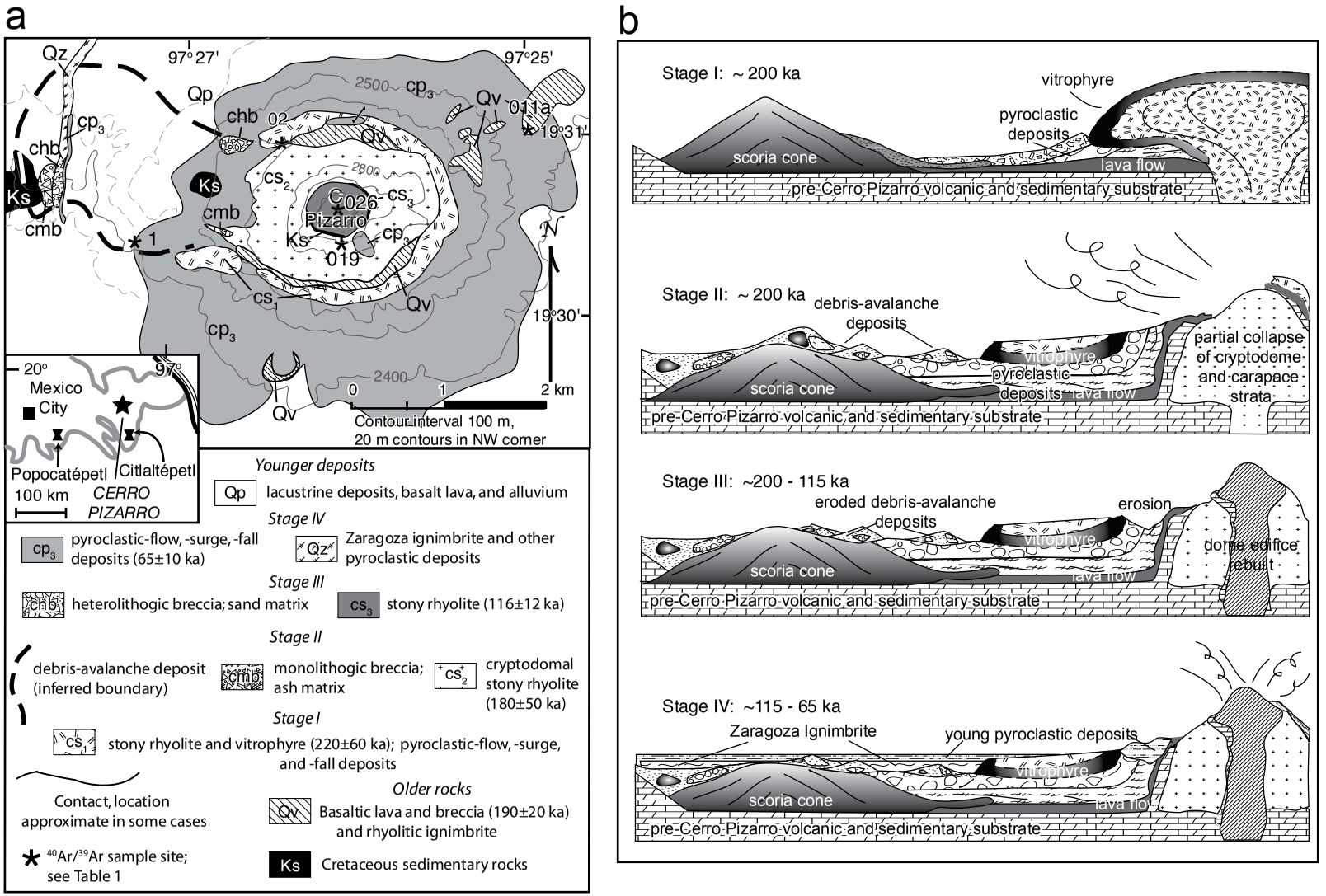

Figura 3. Geology of the Cerro Pizarro rhyolitic dome dome (a), and summary of its evolutionary stages (b) (after Riggs and Carrasco-Núñez, 2004).

trophyric carapace and interior parts of the dome (Figure 4). The distinctive ring that surrounds the dome core is the result of distortion of the first-stage deposits by emplacement of the cryptodome. A large sector collapse left the horseshoe shape seen on the west side of Cerro Pizarro and emplaced a debris avalanche that is best exposed ~2 km to the west of the volcano.

A hiatus of ~60 ka was marked by canyon cutting and reworking of the debris avalanche. The present conically shaped dome was emplaced during this time, but no pyroclastic deposits are confidently associated with this third stage.

Stage four is characterized by pyroclastic eruptions dated at 65 ka and includes a second, long hiatus. Deposits from these eruptions overlie reworked debris-avalanche deposits and the ~100 ka Zaragoza ignimbrite from Los Humeros caldera (Carrasco-Núñez and Branney, 2005). The pyroclastic sequence includes two distinctive marker beds that Carrasco-Núñez and Riggs (2008) showed are exposed in a circular pattern centered around the cone.

Rhyolite domes are considered monogenetic and short lived. The reactivation of Cerro Pizarro after long periods of quiescence is extremely unusual and carries implications for hazards assessment. Likewise the kinds of activity, including Plinian fall and surge deposits and a collapse event, reinforce the idea that a relatively simple model, in which vent clearing is followed by passive emplacement of a dome, is not acceptable for some volcanoes. Riggs and Carrasco-Núñez (2004) speculated that the isolation of Cerro Pizarro has an effect on the unusual behavior. Distance, age, and geochemistry all support the hypothesis that larger volcanoes in the area, such as Los Humeros, are not controlling activity at Cerro Pizarro. Dome eruptions in the TMVB, or any district where rhyolitic domes seem to erupt in isolation from other, larger systems, will serve as an excellent test to assess the apparent severe hazards associated with these small volcanoes.

Alchichica crater (axalapazco)

Alchichica is a crater lake (Laguna de Alchichica) with a quasi-circular shape about 1.8 km in diameter forming an asymmetric tuff ring with a higher profile towards the western rim (Figure 5). It is the largest and deepest crater lake in Mexico with over 60 m deep and is bowl-shaped with a somewhat steeper slope at the southeast. Alchichica belongs to the system of salty endorheic lakes together with other such as: Atexcac, Quechulac, La Preciosa, Tecuitlapa, and Aljojuca. Alchichica and Atexcac are saline (alkaline) in contrast to the other ones that are fresh. The Alchichica lake, along the shoreline,S is characterized by masses of white carbonate microbiolites of several meters that emerged at the lake level due to progressive lowering of that level (Kazmierczak *et al.* 2011). Several littoral benthic macroinvertebrates live in this lake, the species richness in this that is, the saltiest lake in the Serdán-Oriental area, is due to the presence of aquatic vegetation (Alcocer *et al.*, 1998)

Alchichica is one of the largest maar volcanoes (tuff ring) in Mexico. Neverthless it has not been explored in detail. Preliminary geologic studies indicate that

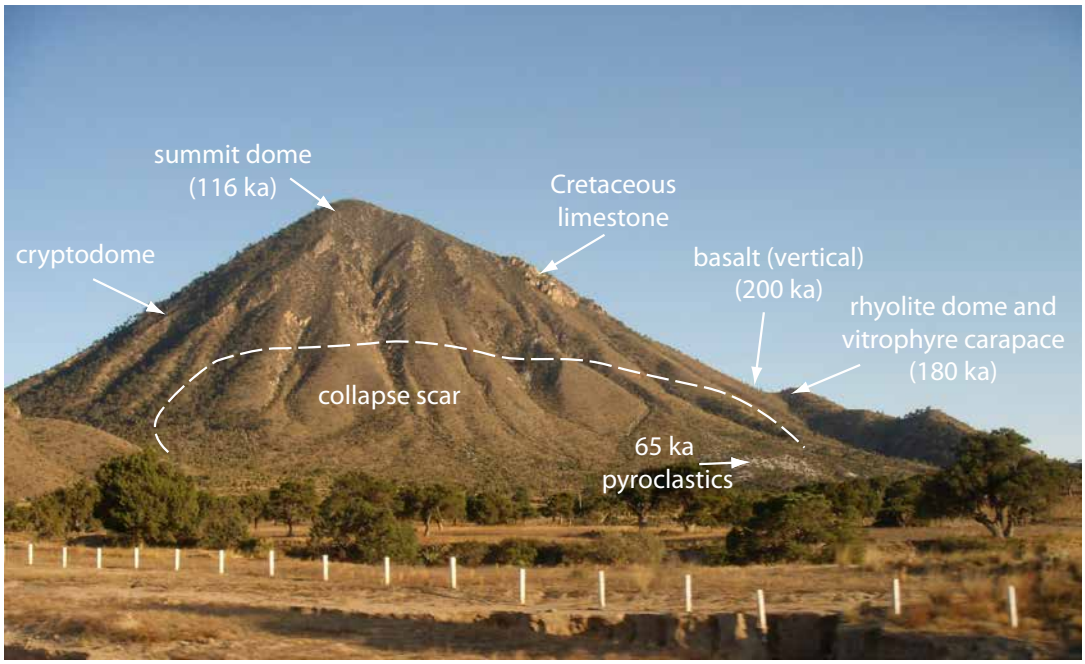

Figure 4. Panoramic northwest view of the Cerro Pizarro rhyolitic dome, showing the different components and ages associated to the complex evolution of this dome. Photograph taken near the Stop A.1.

Figure 5. Panoramic view of highest relief of the Alchichica crater towards the west, where the section depicted in Figure 6 was made.

the Alchichica crater was formed during the transition from magmatic mostly explosive eruptions that constructed a small scoria cone, which suddenly changed its behaviour with the arrival of external water to produce intense pulsating phreatomagmatic eruptions that in turn generated a surge-dominated sequence with abundant ballistic bombs. The lower and medial part of the maar-forming sequence are depicted in Figure 6.

Cerro Pinto tuff ring-dome complex

Cerro Pinto is a Pleistocene rhyolite tuff ring-dome complex (Figure 7) composed of four tuff rings and four domes that were emplaced in three eruptive stages marked by changes in vent location and eruptive character.

The evolution of Cerro Pinto includes three distinct stages (Figure 8) (Zimmer, 2007; Zimmer *et al.* 2010). During Stage I, vent-clearing eruptions produced a 1.5-km-diameter tuff ring (southern) that was then followed by emplacement of two domes (I and II) of approximately 0.2 km^3 each. With no apparent hiatus in activity, Stage II activity initiated with the explosive formation of a tuff ring ~2 km in diameter adjacent to and north of the earlier ring. Subsequent Stage II eruptions produced two smaller tuff rings nested within the northern tuff ring as well as a small dome that was mostly destroyed by explosions during its growth. Stage III involved the explosive evacuation of a small crater and the emplacement of a 0.04 km^3 dome within this crater. Similar to Dome II, Dome IV uplifted and deformed previously emplaced tephra deposits.

Cerro Pinto's eruptive history includes sequences that follow simple rhyolite-dome models, in which a pyroclastic phase is followed immediately by effusive dome emplacement. Some aspects of the eruption, however, such as the explosive reactivation of the system and explosive dome destruction, are rarely documented in ancient examples. These events are commonly associated with polygenetic structures, such as stratovolcanoes or calderas, in which multiple pulses of magma initiate reactivation. A comparison of major and trace element geochemistry with nearby Pleistocene silicic centers does not show indication of any co-genetic relationship, suggesting that Cerro Pinto was produced by a small, isolated magma chamber. The compositional variation of the erupted material at Cerro Pinto is minimal, suggesting that there were not multiple pulses of magma responsible for the complex behavior of the volcano and that the volcanic system was formed in a short time period.

The variety of eruptive styles observed at Cerro Pinto reflects the influence of quickly exhaustible water sources on a short-lived eruption. The rising magma encountered small amounts of groundwater that initiated explosive eruptive phases. Once a critical magma/water ratio was exceeded, the eruptions became dry and sub-plinian. The primary characteristic of Cerro Pinto is the predominance of fall deposits, suggesting that the level at which rising magma encountered water was deep enough to allow substantial fragmentation after the water source was exhausted. Isolated rhyolite domes are rare and are not currently viewed as prominent volcanic hazards, but the evolution of Cerro Pinto demonstrates that individual domes may have complex cycles, and such complexity must be taken into account when making risk assessments.

SECTION A
N-W REGION OF ALCHICHICA

Unit IV

a) Sequence of 30 cm thick of medium grained lapilli of 4-5 cm, alternated with beds of 1-2 cm of ash with juvenile lithics, b) stratified and deformed sequence of 70 cm, dominated by blocks of 60 cm to 1 m, and alternated with laminated horizons of fine ash dominated by balistic activity, c) bed of 80 cm composed of coarse grained lapilli to blockso of fall deposit,composed of juvenile material, d) stratified and deformated sequence of 3 m thick, composed of coarse grained lapilli to blocks of 4-5 cm, alternated with fall deposit of 5 cm thick, of fine to medium grained lapilli, e) stratified sequence of fine grained lapilli, intercalated with coarse grained ash, with medium grained lapilli juvenile material.

Unit III

a) Deformed sequence of 30 cm thick with alternated beds of fine to medium grained lapilli, composed of dark lithics with size of lapilli to blocks, b) diffuse stratified sequence of 1.10 m thick of coarse lapilli to blocks, alternated with very consolidated and laminated fine ash but dominated by balistic activity, c) stratified and deformed sequence of coarse lapilli and blocks, alternated with fall deposits of fine to medium grained lapilli of 10 cm thick, d) stratified sequence of 1.0 m thick of alternated beds of medium grained lapilli with fine grained lapilli, composed of juvenile material, and some blocks.

Unit II

a) Stratified sequence of 2.8 cm thick, of medium to coarse grained lapilli composed of juvenile lithics and oxidized basaltic lava flow, which is intercalated with medium grained ash deposits, b) stratified sequence of 1.40 cm thick, composed of coarse lapilli alternated with fine ash of 1-2 cm thick, with lithics of juvenile lapilli, oxidized basaltic lava flow, “red“ and dark lavas which vary from 1 mm-to block size, c) alternated stratified sequence of 1.9 m thick of fine of 2 cm, medium of 5 cm and coarse lapilli of 12 cm, and some blocks.

Unit I

The base of the section is composed of a a) massive deposit of basaltic scoria of 150 cm, intercalated with a white argillaceous bed of 5-10 cm. This sector is followed by b) fine to medium ash deposit of 35 cm thick, with poor sorted lithics of basaltic scoria and lava flow of 5-20 cm, overlain by a c) coarse grained and poor sorted breccia, which is matrix supported composed of coarse ash, with lithics of basaltic lava flow, and oxidized basalt, d) alternated stratified sector of fall deposit and gray coarse ash.

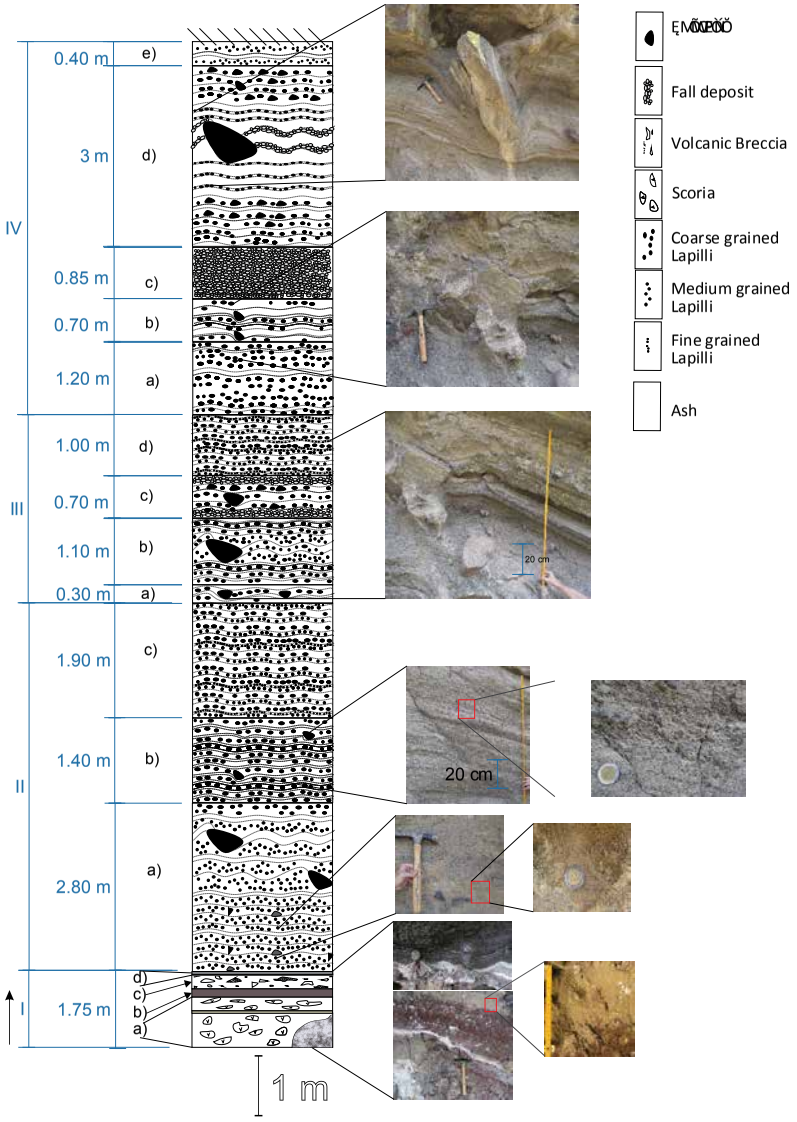

Figure 6. Description of the lower stratigraphic maar-forming sequence of Alchichica crater, in the contact with the underlaying scoriaceous deposits.

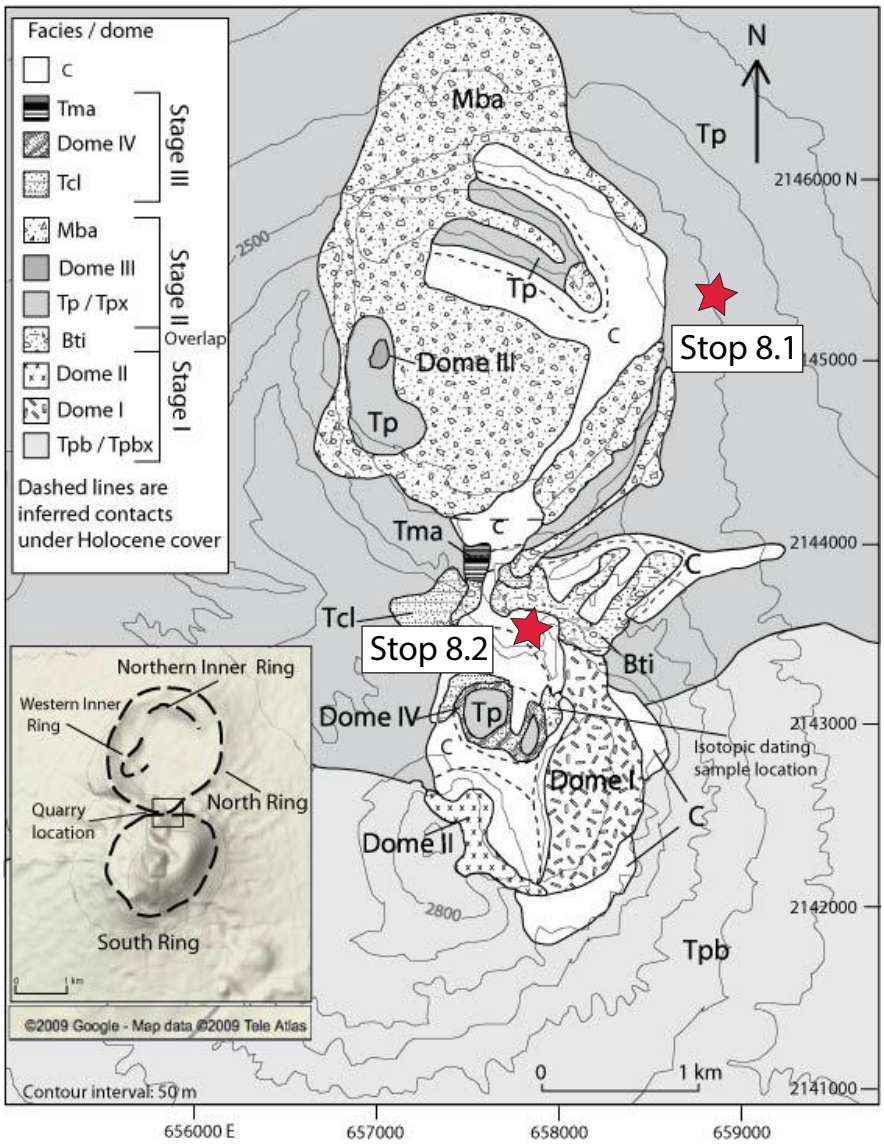

Figure 7. Geologic and facies map of Cerro Pinto Dome Complex (Modified from Zimmer *et al.* 2010). On the main map, the main eruptive stages and associated facies are designated with their distributions shown. The box on the lower left hand-side is a digital elevation showing the four tuff rings generated during the eruption. The main eruptive stages were proposed, which group all the identified facies.

Atexcac maar (axalapazco)

Atexac, with its emerald green lake, is one of the most beautiful craters in the SOB. This crater was excavated into country rock comprising pyroclastic deposits (Figure 9), basaltic lava flows and the eastern flanks of a scoria-cone, which in turn overlie folded limestone rocks of Mesozoic age (Figure 10). The crater is about 120 m deep, with diameters ranging from 1150 to 850 m, elongated to the ENE with beds dipping outward at 16–22º, and the water depth is about 40 m. The pre-eruptive ground surface is about 60 m below the crater rim.

The evolution of the Atexcac crater includes several eruptive stages inferred from a detailed stratigraphic column (Romero, 2000; Carrasco-Núñez *et al.*,2007) (Figure 11). Following an initial short-lived phreatic explosion at the southwest part of the present crater, an ephemeral open-vent vertical column formed. Incorporation of external water led to shallow explosive interactions with the ascending basaltic magma and produced a surge-dominated sequence with numerous sedimentary structures including cross-bedded layers, bomb sags, channels, a few dune forms and layers with accretionary lapilli. After this wet phase, repetitive injection of basaltic magma produced drier explosions, which progressed downward and/or laterally northward, sampling subsurface rock types, particularly intrusive, limestone and andesitic zones. Migration of the eruptive locus and possibly simultaneous eruptions from different vents may have occurred. Also, different degrees of fragmentation are

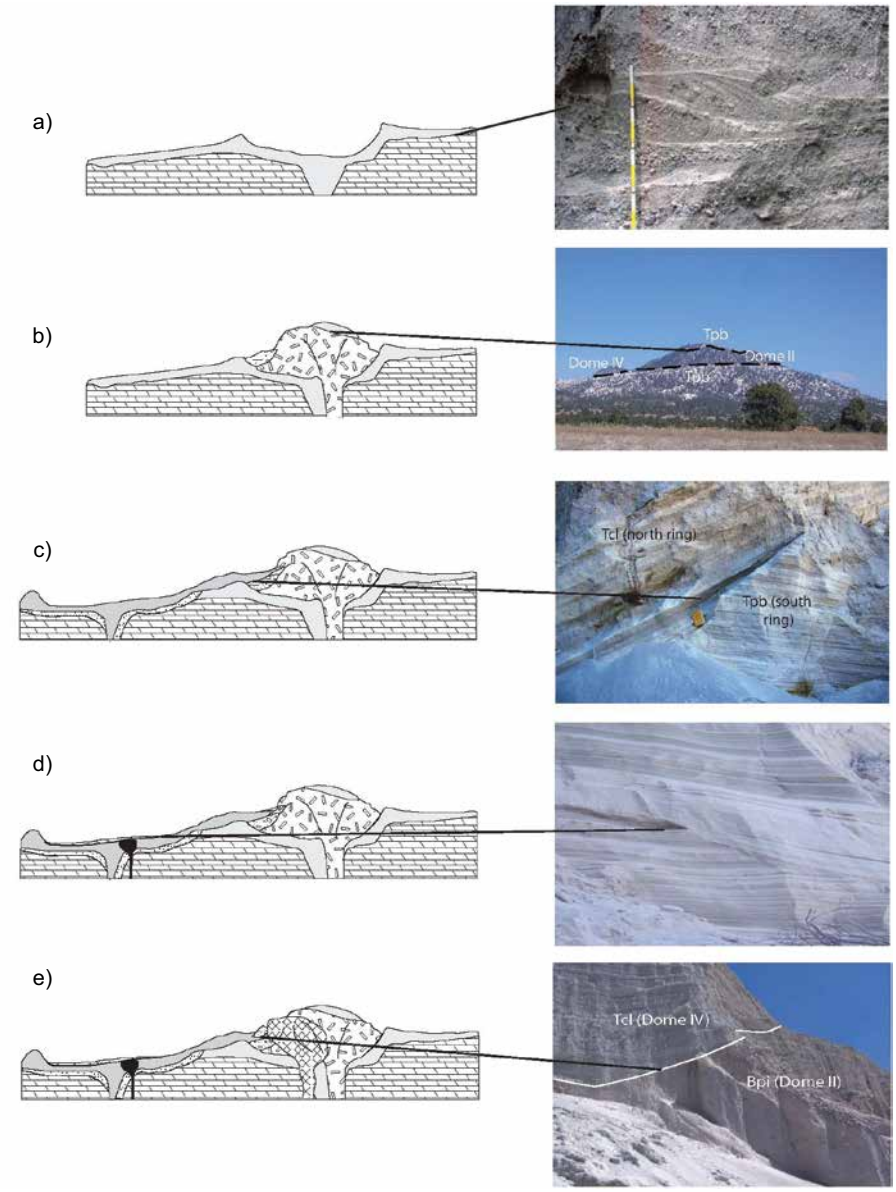

Figura 8. Summary of the evolution of the Cerro Pinto Dome Complex (from Zimmer *et al.*, 2010). A. Stage I- excavation of the southern tuff ring. B. Emplacement domes I & II at the end of Stage I within the ring. The picture shows Cerro Pinto's profile from the west, looking east. Uplifted Stage I tephra caps the domes. C. Stage II- formation of the northern tuff ring, with abundant block-sized flows. The photo shows onlapping of pyroclastics from Stage II pyroclastics on top of the basal pyroclasts from Stage I. D. Stage II- two nested tuff rings were formed within the north ring and the emplacement and inmediate destruction of a small dome (Dome III). Photo shows the contact between deposits of the nested rings. E. Stage III- formation of a crater within the south ring followed by the emplacement of Dome IV. Photo shows the unconformable contact between pyroclasts from the crater explosion overlayinggrain flow deposits.

inferred to produce abundant small andesitic clasts in the S-SW upper deposits at the time large intrusive and limestone blocks were sampled. A final explosive phase involved both a new injection of magma and influx of external water and wetter conditions at the end of the maar formation.

The Atexcac crater was formed by vigorous phreatomagmatic explosions showing strong fluctuations in the availability of external water, temporal migration of the locus of the explosion, and periodic injection of new magma. Carrasco-Núñez *et al.* (2007) infer that the aquifer is dominated by fractured rocks (mostly andesitic lava flows, limestone, and minor intrusive rocks), which contrasts with nearby maar volcanoes, where the aquifer is dominated by unconsolidated tuffs.

Tepexitl rhyolitic tuff-ring (xalapazco)

Tepexitl is unusual because it is a rhyolitic maar. It is about 1 km in diameter, rim to rim, with a crater

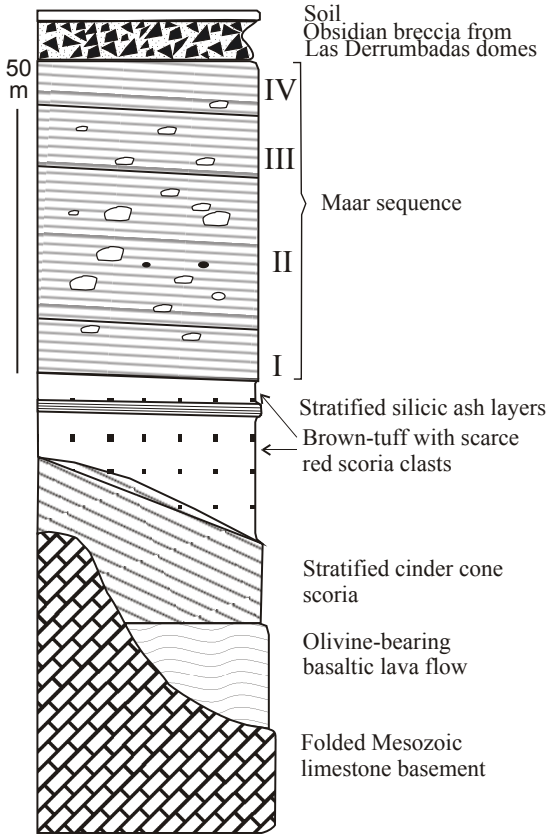

Figure 9. Summary of the stratigraphy of the Atexcac crater (after Carrasco-Núñez *et al.*, 2007). Pre-maar stratigraphy includes Mesozoic sedimentary rocks, overlaid by the construction of a cinder cone, a basaltic lava flow and volcanogenic sediments. The maar-related deposits are grouped into four different units. Post-maar deposits are obsidiane breccia from the nearby Derrumbadas domes.

floor that lies about 20 m below the surrounding peneplain and ~75 m below the maar rim (Figure 12). Active cultivation has covered any outcrops that may have existed on the crater floor and outside the maar, so the contact of the maar deposits with the pre-existing sediments has not been found. Crater-wall deposits are dominated by poorly cemented to nonlithified laminae and fine beds of fine to coarse tuff, with sharp contacts between beds.

The circular form of the maar disguises a complication: the eastern and western halves of the maar have distinct stratigraphic sequences (Figure 13). The eastern crater-walls are moderately well indurated with steep slopes composed of very well exposed, thinly bedded tuff deposits that can be individually traced around the eastern crater rim. The outer apron around the eastern half of the tuff ring also has steep drainages that expose primary sections of bedded tuff, which can be correlated to the inner crater units. The eastern half of the inner crater is also characterized by a 200-m-long, 15-m-high flat-topped ridge extending out from the SE crater wall (Austin-Erickson *et al.*, 2011). The slopes of the western inner crater walls and outer apron deposits are not as steep, and are covered with vegetation and dominantly juvenile float debris, a combination that largely obscures any bedded tuff beneath it. The only visible bedded deposits occur as lapilli breccia in the uppermost 5 m near the inner crater rim (upper sequence unit U3), but cannot be correlated to beds in the eastern half of the crater. Additionally, large concentrations of fragmented breccia bombs and other distinct block textures are found in drainages around the western inner crater. Notably, the flat-topped ridge on the east side is also covered in similar debris and blocks.

Figure 10. Panoramic photograph of the Atexcac crater´s interior. View to the north showing the relations of country rocks: folded limestone, in the lower central part, underlies a cinder cone, which in turn is overlaid by pre-maar deposits (Toba Café) and the stratified maar-sequence atop.

Figure 11. Representative stratigraphic section of the southern wall of the Atexcac crater (Carrasco-Núñez *et al.*, 2007).

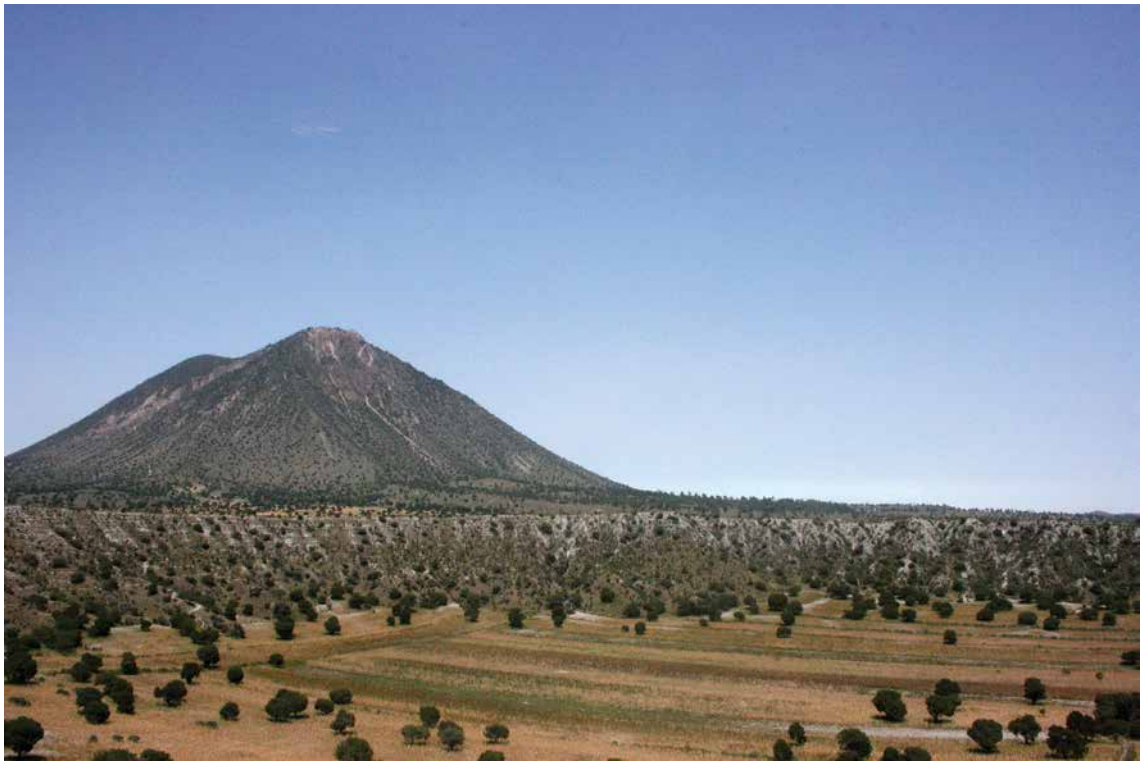

Figure 12. Photo showing the low relief morphology and shallow crater of the Tepexitl rhyolitic tuff-ring. It is aligned NW to Las Derrumbadas rhyolitic domes that appears in the background.

Juvenile material is peraluminous rhyolite (74–75% SiO2) and is poorly phyric (3–7 vol. % phenocrysts), with crystals that vary in size from 0.05 to 0.4 mm. Phenocrysts are dominated by quartz (35–40 vol.%) and plagioclase (30–40 vol.%), with sparse biotite and sanidine (each 10–20 vol.%) and accessory almandine. Juvenile textures are variably dense and devitrified with low vesicularity (herein called 'stony rhyolite', 20 – 25 vol.% vesicles), vitrophyric ('obsidian'), perlitic, brecciated, and flow-banded, with few pumiceous textures. Lithic clasts occur in different proportions throughout Tepexitl's deposits, and are consistent with Toba Café material (Austin-Erickson, 2007). The lithic clast compositions are predominantly recycled local volcanic clasts: andesite, basalt, altered rhyolite, and pumice, with a minor proportion of limestone clasts. Xenocrysts are smaller than 0.5 mm and include rounded sanidine, quartz, tourmaline, hornblende, and pyroxene crystals.

The 'surface debris deposit' on the western slopes of the tuff ring is up to several meters thick, massive, clast-supported with an ashy matrix, monolithologic, and has an average clast size of 10 cm, with a range of 3–80 cm. The deposit is dominated by juvenile material, with breadcrust textures and jig-saw fracturing common. In isolated outcrops within drainages of the western inner crater, the deposit is pink in color, a feature that affects both large and small clasts alike. The underlying thinly bedded, fine-ash to fine-lapilli tuff is rarely exposed in eroded drainages. We interpreted this as a primary deposit that represents the final activity of the eruptive sequence.

The uppermost feature of the western crater surface deposits are large juvenile blocks that litter the slopes and drainages and have textures not observed elsewhere in the stratigraphic sequence, including friable, breadcrust pumice clasts, fractured blocks of cemented juvenile-lithic matrix-supported breccias ('peperite bombs'), and fragmented perlite blocks. The dominant block type is angular stony rhyolite up to 2 m in diameter.

The peperite bombs consist of angular, cemented chunks of matrix-supported, polylithic breccias that contain clasts of dominantly angular to rounded juvenile clasts and minor lithic clasts (Toba Café material, Austin-Erickson, 2007). Some clasts appear to be imbricated within the matrix and some have glassy rinds. The ashy matrix ranges from yellow to pink to gray. Rare lithic clasts are found as float. Another distinct texture found in the western crater is a veneer of yellow-altered clasts present only on the crater rim (the final deposit of U3).

A nearly complete cross-section of the flat-topped ridge's interior can be seen from its western drainage at the connection point with the inner crater (Figure 14). The basal >10 m consists of a massive, matrix-supported, very-poorly-sorted, polylithic deposit with clasts ranging from 1 mm to 20 cm in size. This is overlain by 1.5 m of laminated to thinly bedded tuff, with alternating fine-ash and coarse-ash deposits with sparse pods to discontinuous thin beds of accretionary lapilli. Rare bombs cause 5–15-cm-deep sags in the deposits.

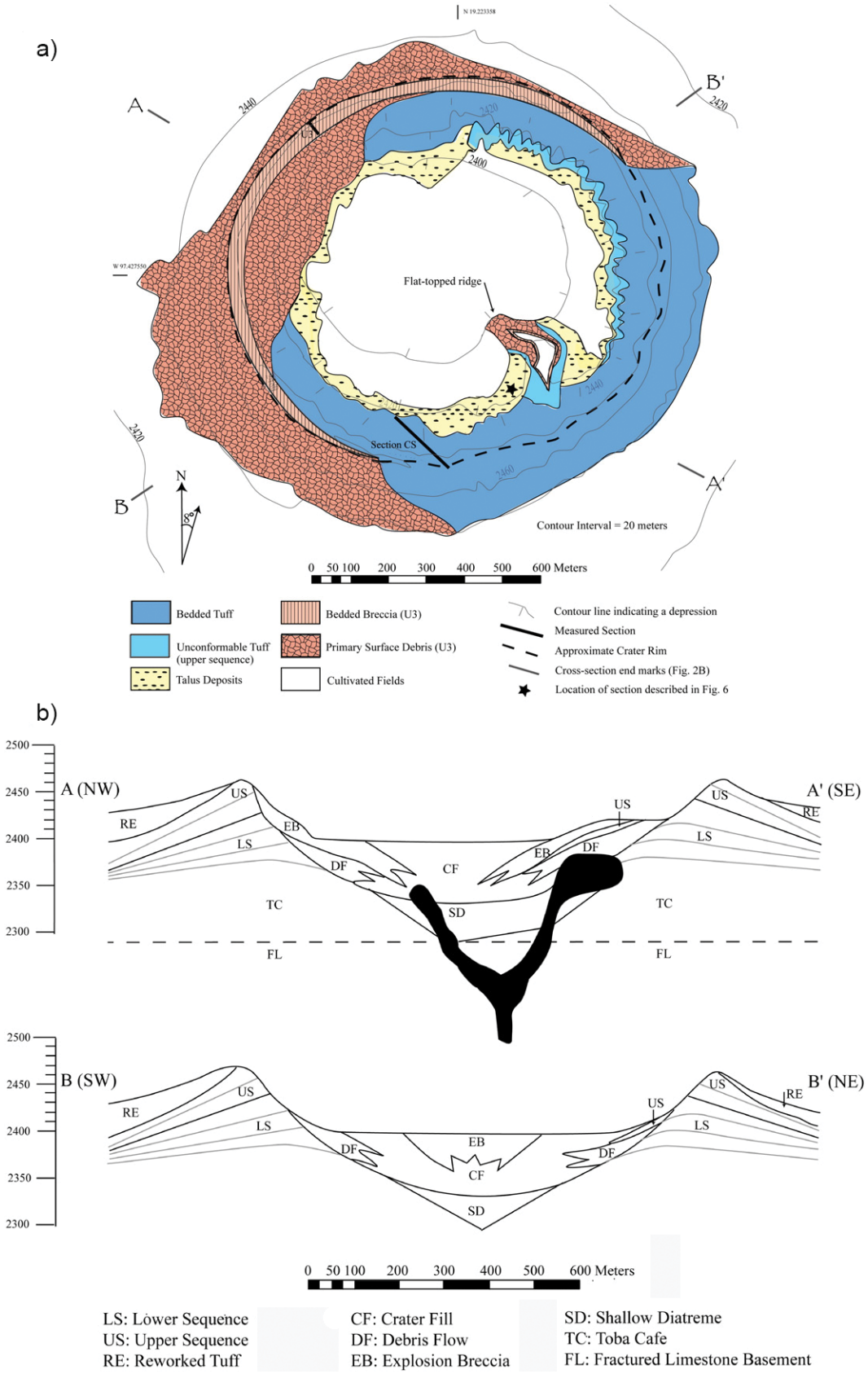

Figure 13. Geological map of Tepexitl tuff ring showing the asymmetric distribution of the deposits and cross-sections showing the interpretation of the different stratigraphic units and the underlying magmatic system as inferred by Austin-Erickson *et al.* (2011).

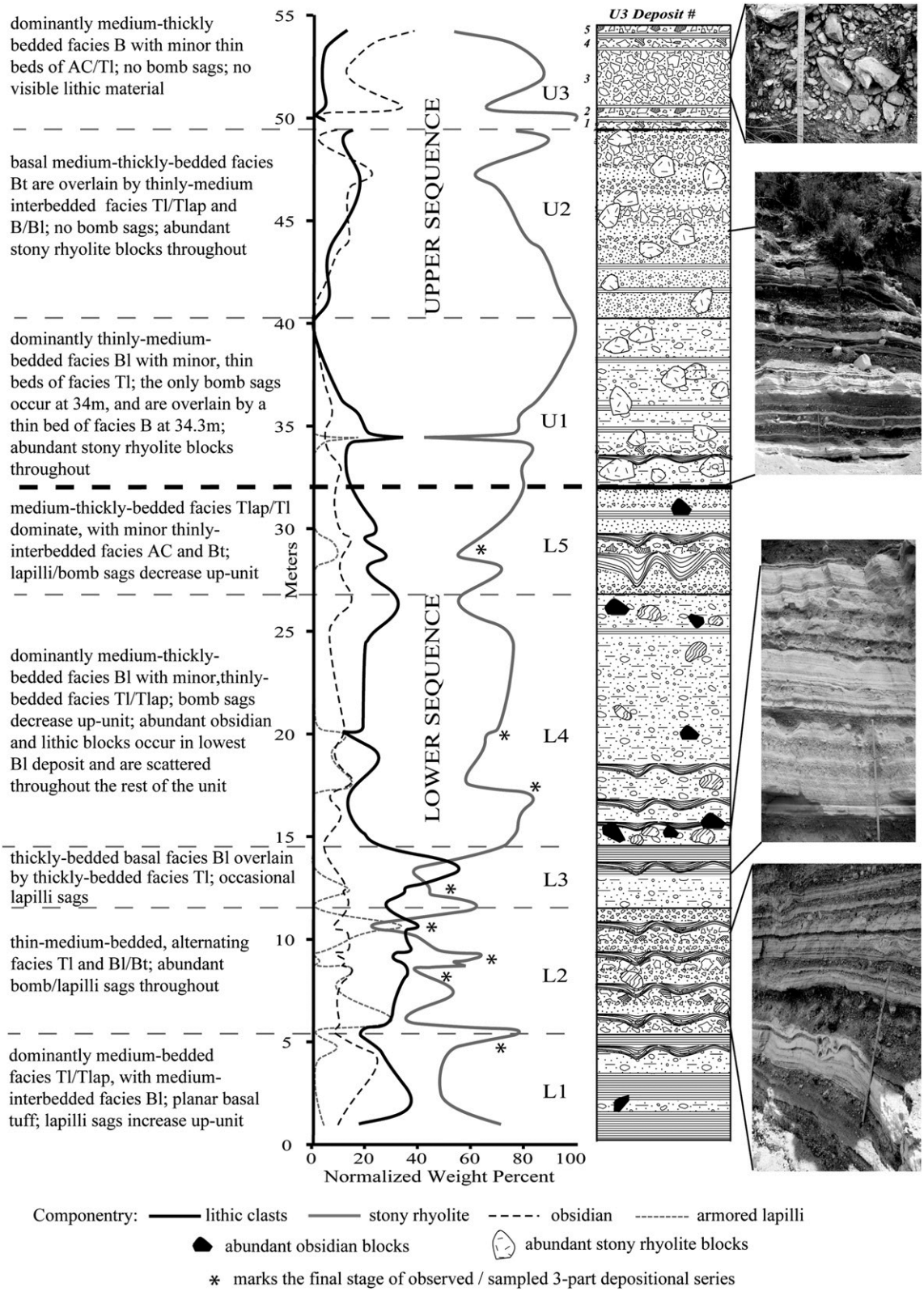

Figura 14. Stratigraphic section of Tepexitl tuff ring showing the two main stratigraphic sequences defined for this volcano (from Austin-Erickson *et al.*, 2011).

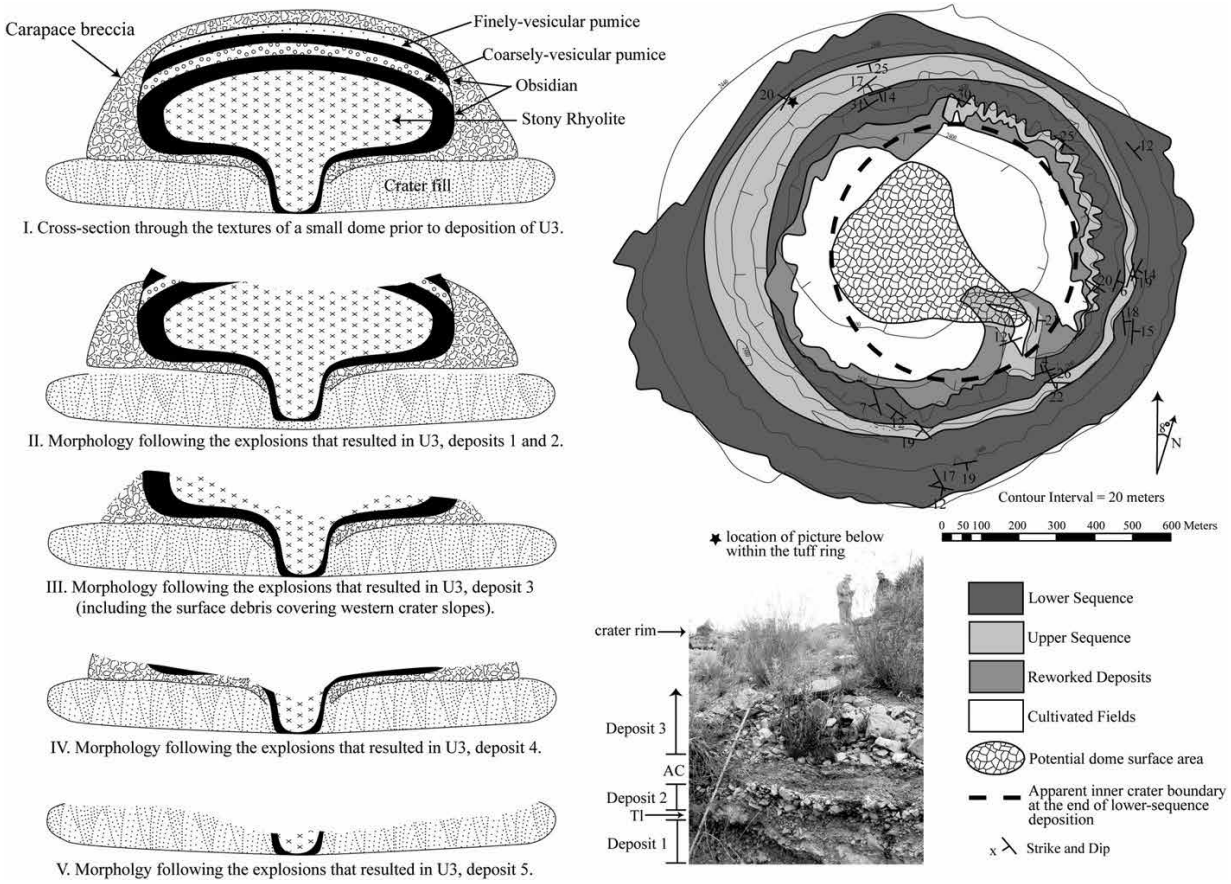

Figure 15. Model proposed Austin-Erickson *et al.* (2011) for the construction and disruption of dome phase during the formation of the Tepexitl tuff-ring.

Overlying this tuff is approximately 1 m of massive, moderately-sorted, clast-supported, fines-poor, monolithologic breccia with angular juvenile clasts from 1 mm to 70 cm in size (dominated by stony rhyolite) — the same as the 'surface debris deposit' that overlies tuff deposits on the western inner crater. This same deposit is also found around the tip of the flat-topped ridge, with an average clast size of 7 cm and isolated patches of pink–red alteration that extend uniformly through the matrix and clasts. Another similarity to the western crater slopes is the high concentration of peperite bombs and friable pumice clasts around the flat-topped ridge. Some clasts found around the ridge have yellow alteration textures, similar to that found along the top of the western crater rim.

Field observations, ash studies (granulometry, componentry, and morphology) and volatile data (LOI and XRF) allow the broad division of the Tepexitl deposits into two depositional sequences (upper and lower) defined by abrupt changes in clast size, dominant facies, block abundance and composition, and apparent water in the system. The lower depositional sequence (5 units; L1–L5) is characterized by fine-grained, accretionary lapilli- and bomb-sag-rich, block-poor deposits, whereas the upper sequence (3 units; U1–U3) is distinguished by coarser-grained, block-rich deposits with no bomb sags. No bedded upper sequence deposits are found beyond the crater rim. Unconformable tuff deposits in the eastern crater and deposits found on and around the flat-topped ridge are also associated with the upper sequence. The upper sequence is thicker in the western half of the crater, along the slopes where the surficial debris is present.

The early eruptions at Tepexitl are interpreted to have been dominated by discrete, highly efficient, phreatomagmatic blasts, which caused a progressive deepening of the eruptive center (lower sequence), followed by a transition to dominantly magmatic behavior in the upper sequence (Figure 15). Rhyolitic dome growth occurred at the end of the eruption, but subsequent retrogressive explosions triggered by external water destroyed all trace of the original dome morphology but left the surface debris deposit on the western crater walls and on the flat-topped ridge.

Molten fuel-coolant interaction (MFCI) is commonly thought to cause the repetitive water–magma interaction in phreatomagmatic eruptions, but a process by which magma and viscous felsic magmas can mingle prior to explosive interaction had not been described. A viable mechanism for rhyolitic MFCI, based upon field work at Tepexitl and laboratory experiments (Austin-Erickson *et al.*, 2008), requires that

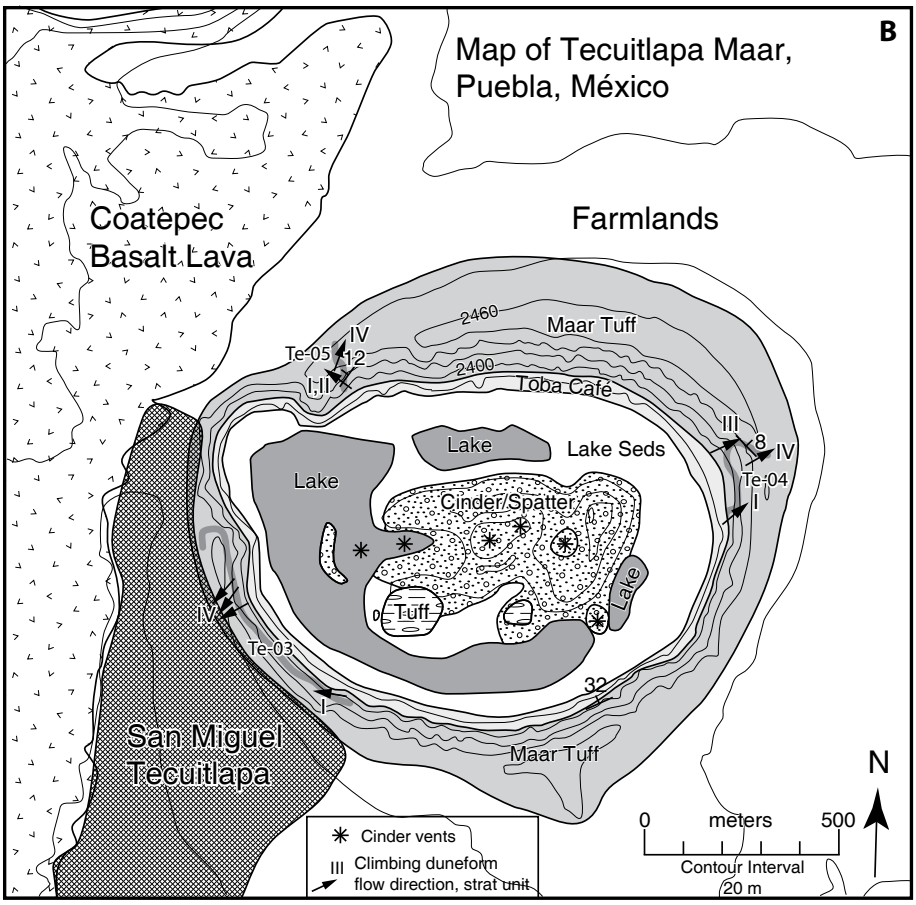

Figure 16. Geologic map of Tecuitlapa maar, from Ort and Carrasco-Nüñez (2009).

fluidized sediments intrude marginal fractures in the rhyolite magma, creating enough interfacial surface area to initiate phreatomagmatic explosions from within the interior of a rising plug or dome.

Tecuitlapa basaltic maar (axalapazco)

Tecuitlapa Maar is a late Pleistocene elliptical basaltic maar about 1.3 km (E–W) x ~1.0 km (N–S) and 100 m deep, excavated about 20 m below the pre-eruptive surface into the toba café (Ort and Carrasco-Núñez, 2009). The toba café, a brown tuff of local volcaniclastic origin found throughout central Mexico, is water-saturated in much of the Serdán-Oriental Basin, with standing water typical during the summer monsoon season. The eruption deposited about 50–70 m of surge and fallout deposits at the maar edge. The crater contains an east–west aligned series of scoria and spatter cones (Figure 16), up to about 70 m above the present maar floor, and a shallow (few m deep) lake fills the western moat. Tecuitlapa deposits are well exposed along the interior rim of the maar, but the surrounding area is covered by post-Tecuitlapa toba café deposits and distal deposits have only been found along a stream northwest of the volcano.

The data from three stratigraphic sections through the maar deposits are most easily interpreted as indicating a locus of explosions that moved from east to west in the maar over time (Figure 17). Thicknesses of beds and maximum grain sizes in the west generally increase, while those in the east decrease, up-section. Dune forms and asymmetric bomb sags indicate a westward migration in vent locations up-section. The facies changes also reflect an approaching (receding) vent in the west (east), as the degree of sorting in the deposits decreases as the explosion locus nears.

The series of scoria and spatter cones inside the maar has an east–west alignment (Figure 18), although individual cones have roughly circular craters. They increase in height and overall volume from west to east, and the overlap of crater borders, with later vents cutting through the rims of earlier vents, indicates a consistently eastward younging direction. The earliest cones formed low-rimmed scoria rings, but later, more easterly cones are tall and conical in shape. Two small (50–100 min diameter) tuff rings and one scoria cone form a lineation parallel to but 200–300 m south of the scoria-cone line. This latter scoria cone deposited ≤2.2-m-diameter spindle bombs within a few tens of meters of the vent. The landforms of these vents blend with those of the neighboring aligned scoria cones, and

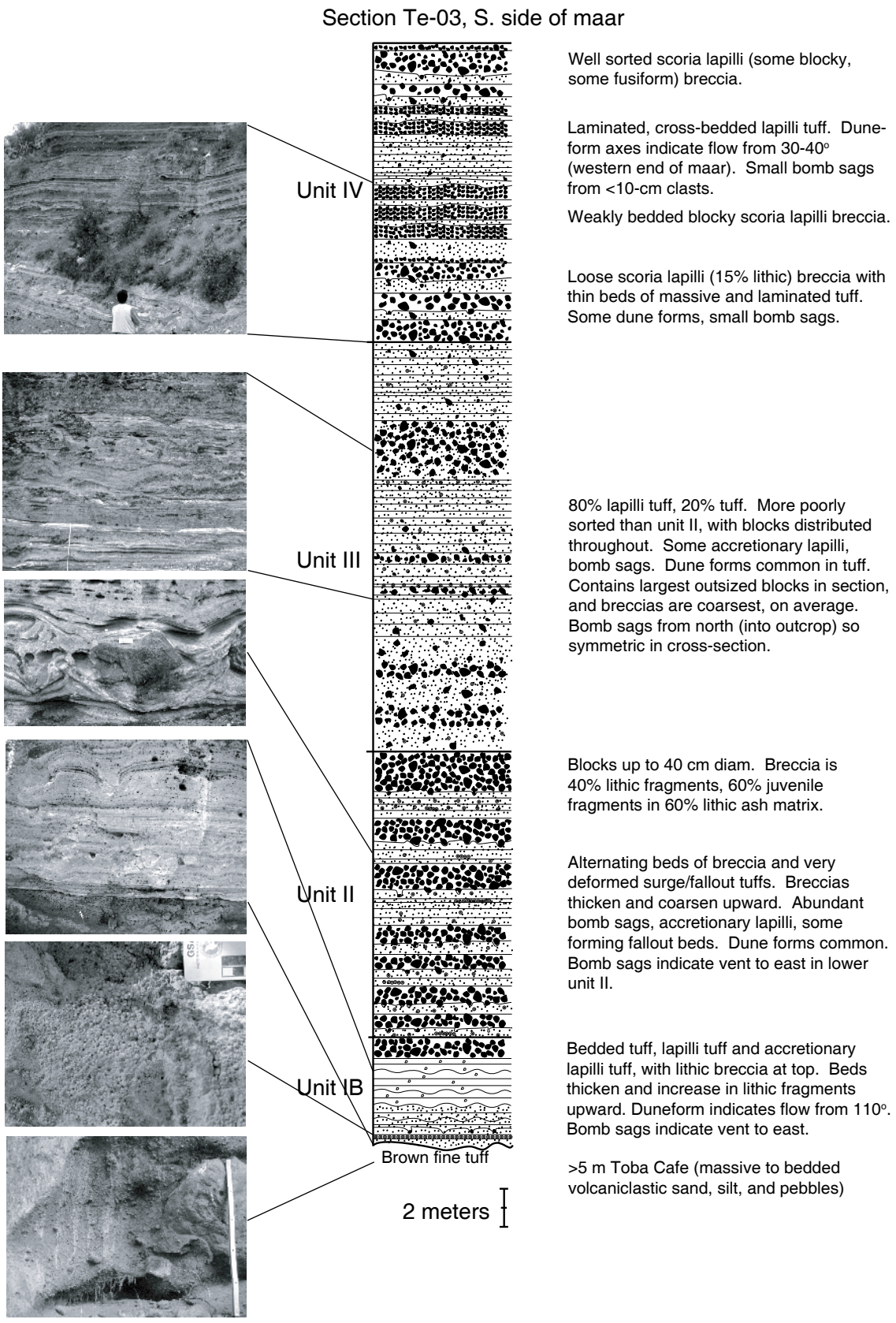

Figure 17. Composite stratigraphic section representative of the southern crater wall of the Tecuitlapa crater (from Ort and Carrasco-Núñez, 2009).

Figure 18. Photo of Tecuitlapa maar from the west, showing the W-E alignment of scoria cones within the crater. The proximal cones appear morphologically more eroded indicating a progression to younging activity towards the east.

may indicate a similar timing for them. This alignment of the scoria cones is similar to those seen at some other scoria eruptions where venting is concentrated at localities along a fissure (*e.g.* La Palma, White and Schmincke, 1999; Tarawera, Houghton *et al.*, 2004; Keating *et al.*, 2008).

In summary, the phreatomagmatic eruption began in the eastern part of the crater, with interaction between the basaltic magma and liquefied tuffaceous sediments. This produced abundant accretionary lapilli as fallout beds and deposits of energetic dilute pyroclastic density currents. The explosion locus gradually moved westward, as evidenced by bomb-sag trajectories, duneform axes, and facies changes, producing an elliptical crater. The eruption then dried out, and began to produce scoria/spatter cones with nested craters that young in age and climb in height from west to east along the same alignment and extent exhibited by the phreatomagmatic eruption. Scoria fall from this portion of the eruption covers the phreatomagmatic deposits along the rim. The lithic lapilli and ash in the deposits throughout the eruption are from the 10–40-m-thick water-saturated toba café, rather than the underlying lavas and limestones.

This eruptive sequence and the lack of any but the shallowest lithic fragments implies that the vent migrated laterally rather than vertically during the eruption. This lack of deepening of the explosion loci may be related to the high lithologic contrast between the non-consolidated sediments and the underlying fractured bedrock. Water movement in the bedrock (fractured limestones and igneous rocks) would have been by fracture flow, whereas movement within the sediments was through liquefaction, failure and fluidization of the deposit. Low magma supply rates would allow collapse of the non-lithified walls of the dike, producing mingling and phreatomagmatic explosions, whereas the same magma supply rate in fractured bedrock may seal off water access to the magma. The alignment of the vents is parallel to regional structural trends, so was probably set in the underlying bedrock, and the distance that the vent migrated is likely related to the overall dike length. The lack of fluidized sediment coating the scoria-cone clasts, both in the cones and in the deposits in the walls of the maar, implies that the phreatomagmatic eruptions used up most of the liquefied sediment, which ended the phreatomagmatic portion of the

Figure 19. Photos of the Aljojuca maar: a) View of the crater interior to the east, showing the underlying pre-maar basaltic lavas and sediments, only the uppermost part correspond to the maar-forming deposits. b) View from the east to see the inward-dipping layers occurred only in that part of the crater. c) Google image showing the W-E alignment of cinder cones with the Aljojuca crater. There is an apparent migration of the volcanic activity towards the west.

eruption. The migration of the scoria-cone vent loci can be explained by an actual migration of the vents, or, because the evidence on their locations is based on surficial crater-overlap relations, by a fissure eruption that closed up from the west to the east, producing later activity at the taller eastern vents.

Aljojuca basaltic maar- axalapazco

The Aljojuca Maar Volcano lies in the Serdán-Oriental basin, and belongs to the South Group of Maars (mexican axalapazcos). It is located at southeastern flank of San Salvador el Seco, between Villa de Aljojuca and San Juan Atenco towns, at Puebla state.

The crater, of probable, Holocene age, has an elliptical shape (Figure 19) of about 1.6 km at the major axis, 0.9 km at the minor axis, and a maximum depth of 50.6 m. Additionally, the crater shows a major elongation to the east, forming an alignment with three scoria cones (E-W) (Figure 19), similar to the dominant fault system for the central Transmexican Volcanic Belt (Suter *et al.*, 1992), which may suggest a progressive migration of the vent along that trend.

The pre-maar rocks in this area are composed of a lower volcano-sedimentary sequence and sedimentary layers, overlain by a vesicular basaltic lava flow, which is in turn overlain by a 0.6 m thick paleosoil and volcaniclastic deposits. The maar-forming eruptive sequence (Figure 20) started with a horizon of 0.7-1.5 m-thick stratified fine ash showing cross stratification with abundant accretionary lapilli of 2-8 mm; b) an alternating sequence, 3.9 m-thick, consisting of poorly sorted breccias and ash beds with some 0.1 m blocks that caused incipient deformation sags; c) a stratified sequence of 6.8 m, dominated by ash beds and some blocks, but without deformation sags; d) a chaotic poorly-sorted and mostly clast-supported massive thick breccia, e) a 9 m-thick stratified se-

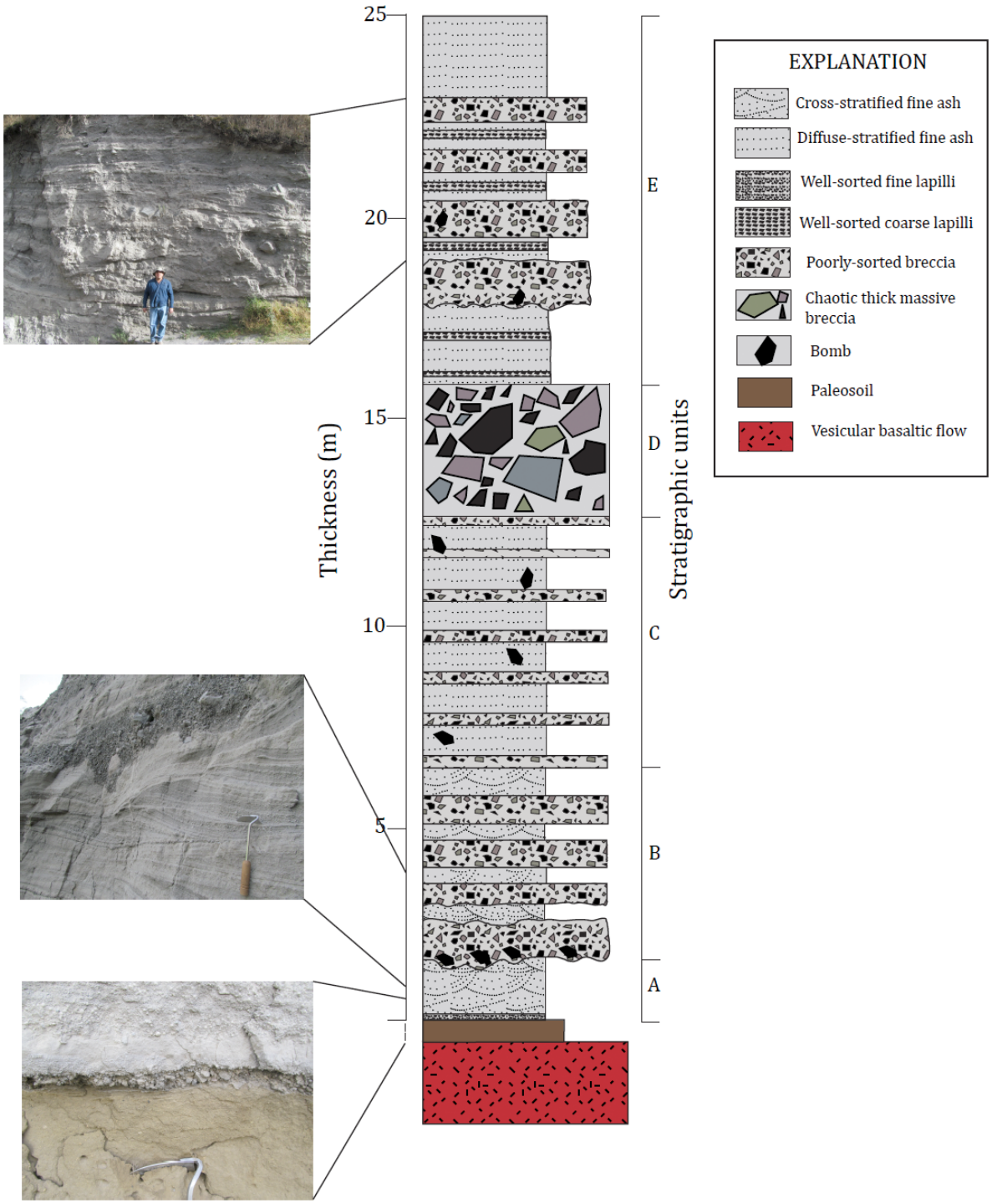

Figure 20. General stratigraphic section of the maar-forming deposits from the Aljojuca maar at the western crater´s wall.

quence, composed of coarse lapilli with ash beds; the thickness of ash beds increases to the top of the sequence.

All previous stratigraphic features suggest a variable explosive activity, from short-lived dry pulses followed by wet layers at the base, and then drier conditions dominated, to finally return to wetter conditions towards the top of the deposits.

ACKNOWLEDGEMENTS

This field guide was funded by PAPIIT grant number IN106810 and Conacyt 150900. Edition of this guide was made by J. Jesús Silva. Logistical support was provided by Centro de Geociencias. Anonymous reviewers provided useful observations that helped to improve this paper.

ITINERARY

Road logs for this field trip guide are provided here; stops for day 1 are labeled with "A", day 2 with "B" and day 3 with "C".

Day 1 (Sunday, November 23)
Basaltic lavas from Los Humeros caldera and Cerro Pizarro rhyolitic dome

Drive from Querétaro to the Serdán-Oriental area (Figure 21). After lunch, visit Cerro Pizarro rhyolitic dome to see avalanche-derived deposits, Zaragoza ignimbrite from Los Humeros and phreatomagmatic surge and fallout deposits derived from Cerro Pizarro. We will visit Holocene basaltic lavas from Los Humeros and then have a brief stop at Cantona archaeological site (Figure 2). Night at Perote.

Road log Day 1 – Stops for Day 1 are shown in Figure 22 and Table 1.

Stop A1
Cerro Pizarro debris-avalanche deposits
Location: UTM 14Q 660948 / 2157749

Debris-avalanche deposits are exposed in an active quarry west of Cerro Pizarro. Exposures change frequently, but several facies can commonly be observed. The breach on the west side of Cerro Pizarro is visible from this location. Jigsaw-fit stony rhyolite and vitrophyre clasts in a matrix of very finely comminuted ash have been documented in past visits; the rhyolite facies are part of the first stage of the dome. At the rear of the quarry, look for a stratigraphic succession that comprises debris-avalanche or reworked debris-avalanche deposits overlain by 100-ka Zaragoza ignimbrite and pyroclastic fall deposits from the 65-ka stage-four eruptions of Cerro Pizarro (Figure 23). Details of the former pyroclastic succession can be explore in several ourcrops nearby (Figure 24).

Stop A2
Rim-fracture lavas from Los Humeros caldera
Location: UTM 14Q 654913 / 2166235

One of the most recent volcanic episodes related to the activity of Los Humeros caldera and geothermal field is associated with the caldera-rim volcanism, which is represented dominantly by blocky and *a'a* basaltic andesite lava flows and minor explosive activity. At least four lava fields were formed along the southern Los Humeros caldera rim, through fractures and small cinder and scoria cones. In contrast with the other basaltic andesite lava flows, the westernmost lava flow is the only olivine basalt. In this stop (A2.1), we will examine the outer structure of this lava (Figure 25), which rests atop a pyroclastic fall sequence derived from plinian to subplinian eruptions generated from the central part of the caldera (Wilcox, 2011). An organic-rich soil cropping out between those units was dated at about 3.5 ky, providing a maximum age for that basaltic lava. A few centuries later, the first settlements were built in Cantona, and in time it became one of the largest pre-Hispanic cities in Mesoamerica, having an estimated population of about 100 thousand inhabitants. Stop A2.2 is at the Cantona museum and archeaological site. Location: UTM 14Q 657647 / 2162423.

Table 1. Road log Day 1.

Km	Directions
0.0	Meet at the Misión Juriquilla Hotel parking lot.
4.6	Merge onto motorway No. 57 southbound toward Querétaro City.
22.0	Drive trough the Querétaro City and continue on motorway 57 southbound to México City.
150.0	Take the junction to Puebla at the Arco Norte motorway Stop at a Gas Station at the right of the road.
300.0	Continue on the Arco Norte highway. Take the exit to Apizaco/Huamantla on road 136, after the second exit to Calpulalpan (Sanctórum Toll Road).
352.0	Pass trough the outskirts of Apizaco and Humantla on road 136.
390.0	Follow signs to Veracruz/Xalapa and merge onto toll road 140D to Perote.
432.0	Pass the tunnel through Cerro Grande mountains and cross into the Serdán-Oriental basin.
444.0	Exit at the toll booth toward Tepeyahualco, cross the town and drive northbound for about 2 km on a dirt road to a quarry and have a panoramic view of Cerro Pizarro from the west. Stop A1. Lunch.
463.0	Drive back to the toll road, cross it to the north toward Cantona archaeological site and right after passing the town of Tecatl, park for Stop A2.1.
483.0	Drive back to Cantona and explore the local museum. Stop A2.2.
493.0	Drive back to the toll road 140D and turn left toward Perote
530.0	Take exit sign-posted Perote on the right-hand side (east).
532.0	Drive 3 km southbound toward the town of Perote and at the major intersection in town, turn right onto road 140 toward Puebla (SW).
533.0	Drive for 1.5 km to Hostería Covadonga Hotel on the left side of the road.

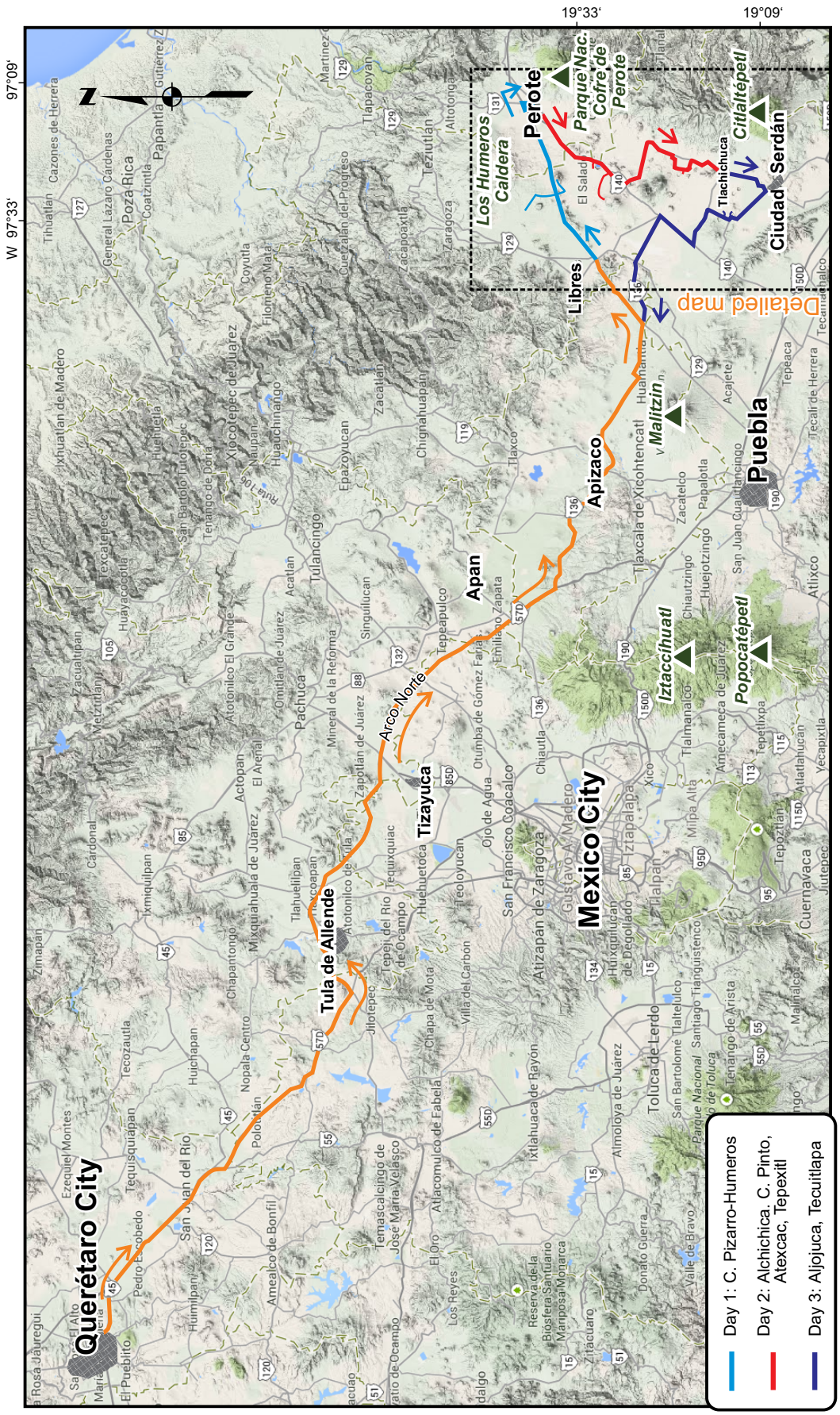

Figure 21. Road map showing the route from the beginning in Querétaro to Perote, and general route for the three-days field trip, marked with a box (orange / light blue – first day; red – second day; and dark blue – third day)

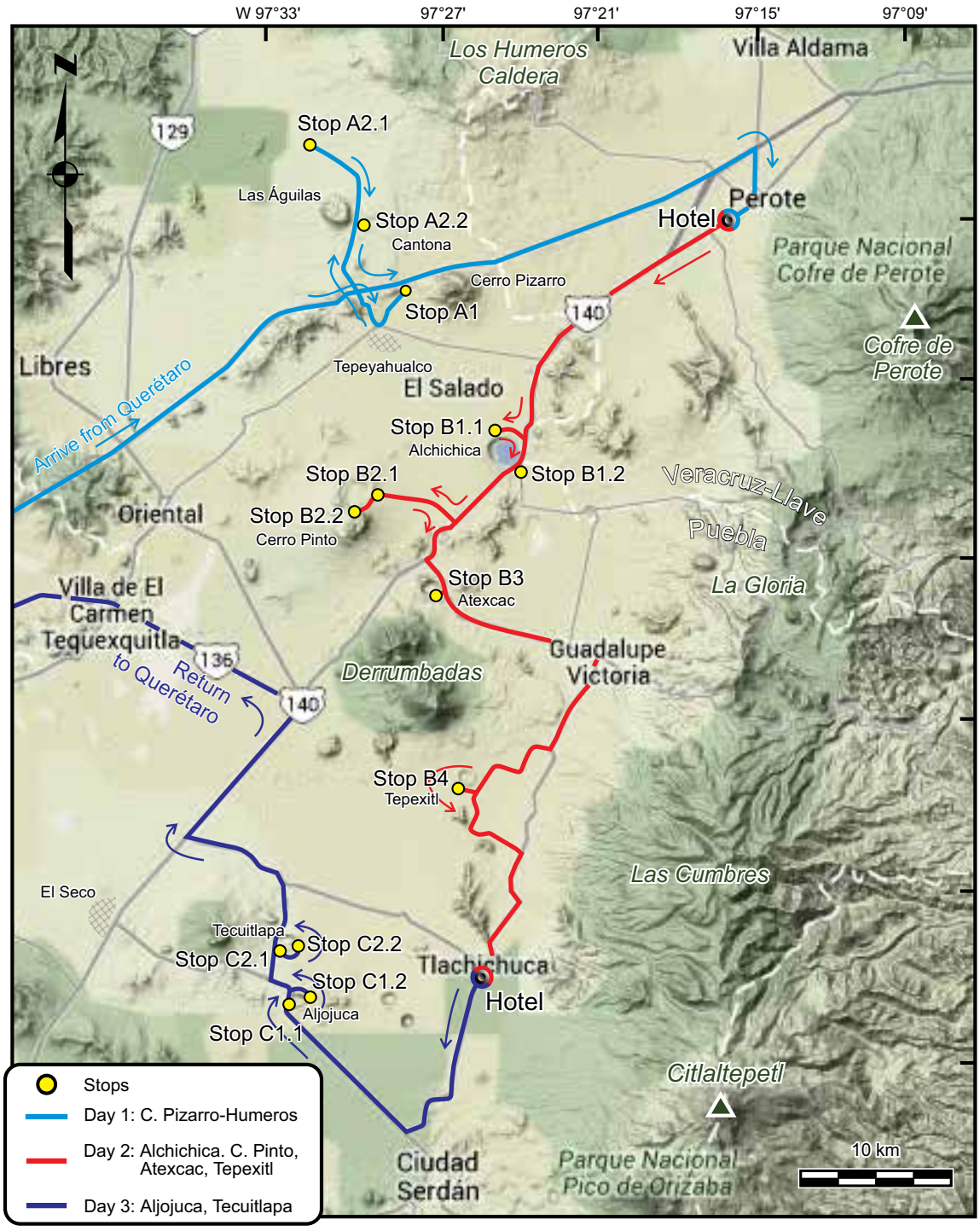

Figure 22. Map showing the route and stops for days 1 (A- in blight blue), 2 (B-in red) and 3 (C-dark blue).

Figure 23. Stop A1. Photo showing vulcanoclastic deposits (at the base) derived from a small sector collapse event associated to the Cerro Pizarro evolution. They are overlaid by the Zaragoza ignimbrite dated at 140 ky (Willcox, 2011), pyroclastic deposits from an unknown source and a thin white pyroclastic layers derived from Cerro Pizarro atop, composed by pumice fall and surge layers, which were dated at 65 ky (Carrasco-Nuñez and Riggs, 2008)

Day 2 (Monday, November 24)
Maars of the central Serdán-Oriental basin

Drive from Perote to the south toward Alchichica crater. Continue to Cerro Pinto, stop at the main quarry to see relations between domes and tuff-ring structures and then stop at the crater rim to see unconformable contacts of pyroclastic sequences. Continue to Atexcac crater and, after lunch, walk to the inner crater. Continue to Tepexitl rhyolitic tuff-ring. Night at Tlachichuca.

Road log Day 2 –Stops for Day 2 are shown in Figure 22 and Table 2.

Stop B1
Alchichica crater

Stop B1.1
Location: UTM 14Q 666765 / 2147767

Corresponds to the western highest slopes of the Alchichica crater, where we will explore the contact between the maar-forming deposits in the abrupt change from the underlying scoria cone, and discuss the transition from magmatic to phreatomagmatic conditions (Figure 26). We will have the chance to see exposures of the emerged microbiolites along the shoreline.

Stop B1.2
Location: UTM 14Q 668556/ 2147044

Driving around the Alchichica crater to the east, we will find where we will see spectacular exposures of sedimentary features such as: bomb sags, soft-sediment deformation in wet layers and lapilli accretional (Figure 27).

Figure 24. Photograph showing part of the surge and fall sequence, at the place where it was dated at 65 ky. Notice the plastic deformation of the upper surge layers.

Stop B2
Cerro Pinto
Location: UTM 14Q 657902 / 2143477

We will drive southbound onto the state free road Perote-Puebla. After about 8 km we turn right toward Izoteno village and then toward Cerro Pinto mountain. General geology and evolutionary stages for Cerro Pinto dome are depicted in Figures 7 & 8. We are entering the North Ring of the complex from the east, slowly climbing the outer flanks. The first stop is at the hinge of the North Ring. From here, we will drive to a quarry located at the center of the complex.

Stop B2.1. crater rim
Location: UTM 14Q 658899 / 2145248

At this road cut stop, you can see the transition from outward dipping deposits to deposits dipping inward toward the vent (Figure 28). Most of the deposits here represent the dry part of Stage II eruption that produced the North Ring. Fallout beds dominate but surge deposits are found sporadically. Cresting the pass and dropping into the North Ring, you can see the ridgelines of the nested inner rings directly ahead and to the north.

Stop B2.2. The quarry
Location: UTM 14Q 657902 / 2143477

The perlite quarry offers excellent exposure into the area at the junction of the North and South Rings.

Figure 25. Stop A2.1. Blocky basaltic lava flow from rim-fracture volcanic activity of Los Humeros caldera This lava overlies thermally altered Holocene soil (ca. 3,200 yr B.P.) and pumice-fall sequences derived from Los Humeros caldera´s activity, which are separated by silty soil-like layers.

Immediately on your left as you enter the quarry is a tall outcrop of interbedded grain-flow and surge deposits (Figure 29). We envision that these deposits were produced as dome material from Dome I and II collapsed, flowing to the north, while surges emanated from the North Ring, interbedding with the episodic grain flows. It is also possible that the tephra was coeval with the grain flows and simply represents settling of a cloud of ash and fine lapilli elutriated from the grain flow. Along the south wall, depending on the most recent excavations done at the quarry, you can often see the unconformable layers of the Stage III explosion crater in cross section.

Stop B3

Atexcac crater

Location: UTM 14Q 663033 / 2138202

A walk along the crater rim to the southeast allows a panoramic view of the western wall of the Atexcac maar crater (Figure 10). Country rock is well-exposed and comprises the highly folded and fractured Cretaceous limestone. forming a topographic high that is covered by the deposits of a basaltic cinder cone and a basalt lava flow dated at 0.33±0.08 Ma by Ar^{40}/Ar^{39} (Carrasco-Núñez *et al.*, 2007). The large abundance of altered andesite (presumably of Tertiary

Table 2. Road log Day 2.

Km	Directions
0.0	Meet at parking lot of the Covadonga Hotel after breakfast at the restaurant. Turn left (SW) and drive to the south onto state road 140 toward Puebla to get Alchichica.
24.0	Drive inside the crater, turn right to the base of the higher peak for Stop B1.1.
26.0	Drive back to reach the southern exit and stop at the crater rim to explore impact structures on wet surge deposits. Stop B1.2.
30.0	Drive on state road 140 toward El Seco-Puebla and, after 6.2 km, turn right (west), pass the village of Itzoteno and continue to the Cerro Pinto quarries to Stop B2.1. After that, continue on the same road for 2.3 km to Stop B2.2.
44.0	Drive back to main road 140 and turn left at the road El Seco-Puebla.
50.0	Drive for about 3.6 km to SW, and turn right heading to San Luis Atexcac Village.
54.0	After 1.8 km, turn right on a dirt road going toward the crater rim and park.
55.0	Walk up to reach the crater rim and walk around to the left; Stop B3.
56.0	Drive back to the main road 140, turn right (SE) toward Guadalupe Victoria Town.
58.0	Pass the town and head to the south for about 7 km, then turn right to take a dirt road toward Las Derrumbadas mountain to the west, then turn left to another dirt road.
83.0	After 4 km, you will see the gente but visible tuff ring morphology, turn right to approach the crater. Park and walk into the inner Tepexitl crater. This is Stop B4.
87.0	Drive back to the paved road Guadalupe Victoria-Tlachichuca, and turn right until arriving to Tlachichuca.

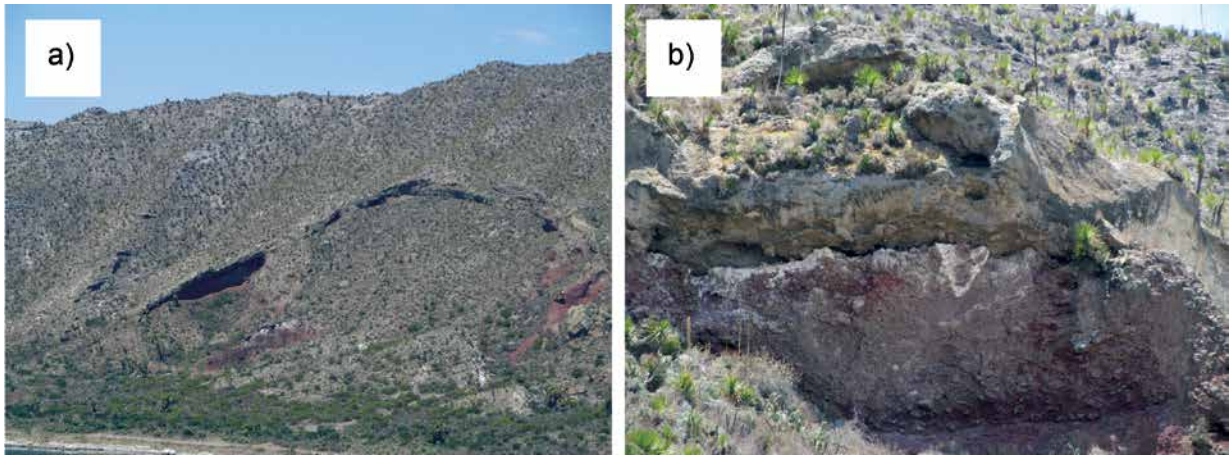

Figure 26. Stop B1.1 a)Photograph of the western highest crater walls of the Alchichica maar showing the deposition of the maar-forming Alchichica sequence over a relatively small scoria cone; b) Photograph showing the contact between the lower scoriaceous strombolian-to-vulcanian deposits overlaid by the maar-forming deposits.

age) within the maar-forming deposits indicates the presence of those rocks underneath the basaltic lavas (Carrasco-Núñez *et al.* 2007). Overlying this is a brown volcaniclastic sediment ('Toba (tuff) Café') that contains volcanic clasts from the Serdán-Oriental basin, which probably represents a protracted period of eolian and fluvial erosion and deposition. Although this tuff is the uppermost aquifer of the basin and is the source of water for most of the phreatomagmatism in the area, in Atexcac the explosions apparently occurred at greater depths. At the uppermost parts of the pre-maar sequence, a thin white rhyolitic fallout tuff is present and correlates with deposits from Cerro Pinto.

On the edge of the crater, we can examine the proximal maar-forming Atexcac sequence, which is characterized by both fallout and surge deposits. Lapilli tuffs and lapilli breccias are common. Layers with accretionary lapilli and ballistic blocks that made bomb sags in the deposits attest to the wet, soft nature of the deposits at that time. An obsidian breccia derived from a collapse event at Las Derrumbadas overlies the Atexcac sequence on the far side of the maar.

At this site, we will discuss the possible trends of eruptive migration and possibly simultaneous eruption from different vents, based on the morphology of the crater, and ballistic impact data. We can also discuss the variations on the depth of explosion, variations of water supply and hydrogeologic conditions of the fractured basement of andesite and limestone,which was likely water saturated, as may have been the thin overlying veneer of 'Toba Café'. We infer that the eruption started in the southwest portion of the crater and migrated to the northeast, before reversing late in the eruption, based on the size and type of lithic and juvenile blocks (Figure 30). However, it is not clear whether the eruption shut off as vents were abandoned during migration, or if the apparent migration is simply due to the relative vigor of eruptions from different parts of an erupting dike.

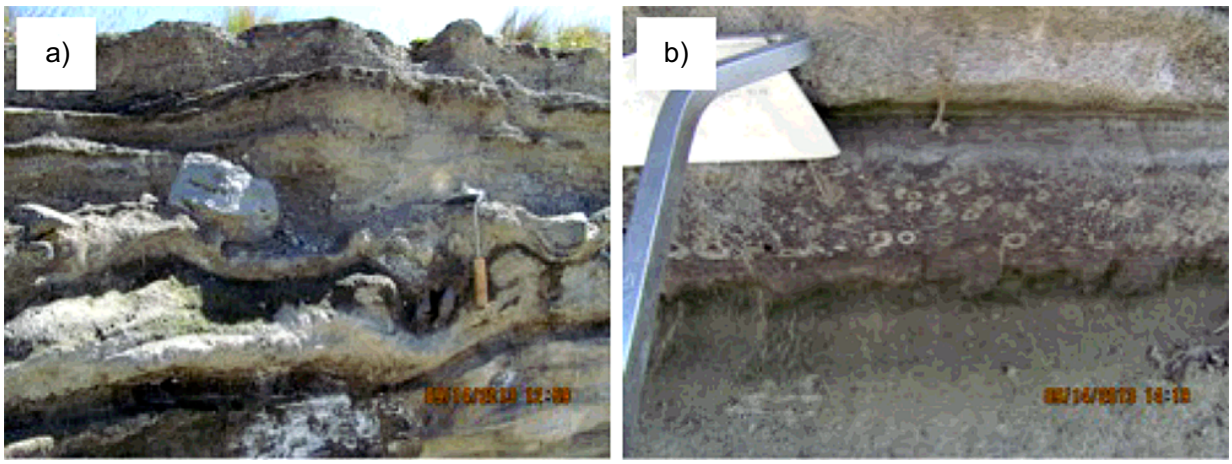

Figure 27. Stop B1.2 a) Photograph showing some examples of multiple ballistic impact structures and different deformation styles of the wet surge deposits at the Alchichica eastern crater´s walls; b) Photograph showing a layer with abundant large accrecional lapilli, which is a very common feature in the Alchichica eruptive sequences.

Figure 28. Stop B2.1 Photograph showing unconformable bedding planes at the hinge of the northern tuff ring. Here beds change dip direction from vent facing to outward facing. The beds were all emplaced when the northern ring was first excavated during Stage II.

Stop B.4
Tepexitl tuff-ring
Location: UTM 14Q 665277/ 2125954

At this stop, we will walk into the crater along a dirt road. We will examine the deposits of the upper and lower stratigraphic sequences. If we have enough time, we will walk to the western rim and inspect the breccias there. This stop will allow us to discuss the interactions of very viscous rhyolitic magma with water and the phreatomagmatic deposits thus produced (Figure 31). We will discuss evidence for the explosive dismemberment of a rhyolitic dome late in the eruption.

Day 3 (Tuesday, November 25): Maars of Lower Serdán-Oriental basin

Drive from Tlachichuca to Aljojuca, view from the southern rim crater and explore maar-forming sequence, then drive into the crater for closer inspection of the pre-maar rocks and upper pyroclastic section (see Figure 14). Drive to Tecuitlapa crater and walk to examine the maar-forming sequence as well as the cinder cones in the inner crater.

Road log Day 3 – Stops for day 3 are depicted in Figure 22 and Table 3.

Stop C1
Aljojuca maar

Stop C1.1. western crater rim
Location: UTM 14 Q 653759 / 2111469

From the western rim of Aljojuca crater we will see a panoramic view of the crater general stratigraphy (Figure 19a) and the alignment with the cinder cones to the east (Figure 19c). At Stop C1.1 we will visit the western section of the maar-forming sequence, starting from a thin scoria fall layers (Figure 20) overlaid by a surge-dominated sequence showing typical cross-bedding stratification (Figure 32a). In this section we

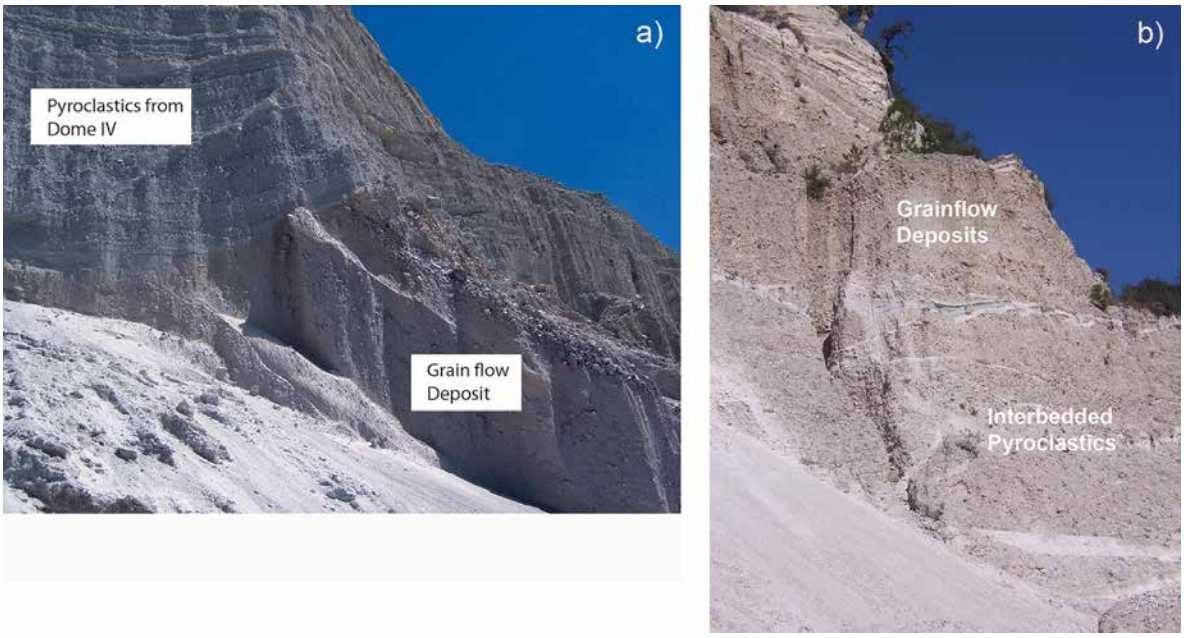

Figure 29. Stop B2.2. Prominent outcrops within the quarry. a) Location along the southern wall of the quarry where pyroclastics from the Stage III crater unconformably overlie preexisting grain flow deposits created as Domes I and II shed material during emplacement. b) Interbedded surge and grain flow deposits along the northern wall of the quarry.

Table 3. Road log Day 3.

Km	Directions
0.0	After breakfast at Casa Blanca restaurant, drive to the south to leave the town toward Serdán town.
16.0	At the junction of road towards El Seco, turn right (NW)
29.0	Drive to Aljojuca Village and park to take a panoramic view of the crater and walk along the rim until Stop C1.1
33.0	Drive around the crater to the left side and, after exploring the upper pyroclastic sequence, go into the bottom of the crater to see the pre-maar rocks. Stop C1.2
40.0	Drive toward El Seco and turn right to enter Tecuitlapa town, cross the town to the end and enter the crater. Stop C2
42.0	Walk along the crater road to explore the whole sequence and drive to the bottom of the crater to visit the recent cinder cones.
43.0	Drive to the north toward San Nicolás de Buenos Aires village and, at the road junction 394, turn left until the intersection with road 140.
60.0	Turn right toward Perote, drive until Zacatepec village and then take road 136 toward Huamantla-Apizaco, drive for 42 km
140.0	Drive for 27.5 km toward Apizaco on road 136
190.0	Drive on road 136 to the junction with toll motorway Arco Norte toward the northwest (Cd. Sahagún).
470.0	Merge with main road 57 México-Querétaro and arrive to Querétaro City (approximately 317 km).

will see the contact of the maar succession with the underlaying country rock composed by basaltic lava flows and a paleosoil (Figure 32b).

Stop C1.2. eastern and crater interior
Location: UTM 14Q 654629/ 2111591

Driving to the opposite side of the crater (east) and going down into the crater is Stop C1.2, where you can see the inward-dipping maar-forming succession in contrast with the sub-horizontal sequence shown in the main crater (Figure 19b). At the lake level, a volcano-sedimentary sequence underlying the basaltic lava flow (country rock) is exposed, indicating the variable conditions of the local aquifer from fractured to granular.

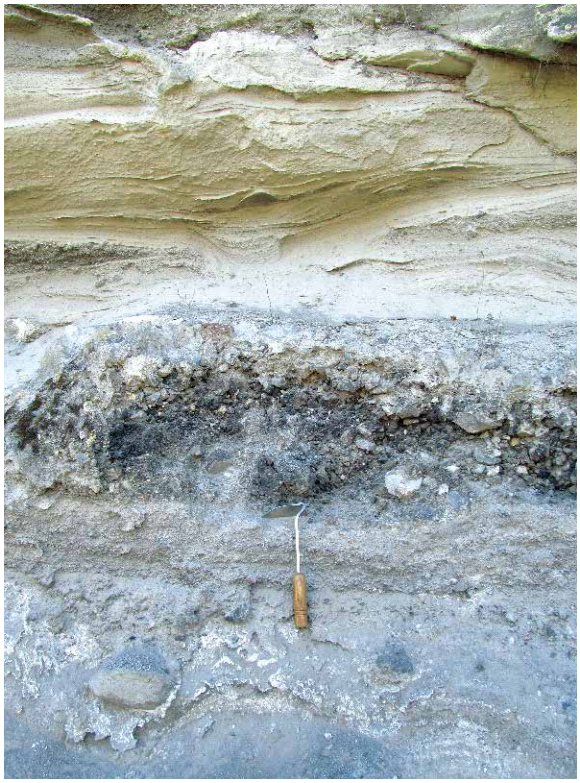

Figure 30. Stop B3. Photograph showing the alternance of cross-bedded surge deposits with juvenile scoriaceous fall layers at the lower part of the Atexcac maar..

Stop C2
Tecuitlapa maar-forming sequence
Location: UTM 14Q 653078 / 2115058

We will make two stops at Tecuitlapa maar. These are along a road that descends into the crater, providing easy access and good outcrops.

Stop C2.1. southwestern crater wall

The first stop is really a long traverse along which we will observe the four main stratigraphic units of Tecuitlapa maar. Spectacular bomb sags are a highlight (Figure 33c). We'll look for evidence of changing vent proximity within the sequence.

Figure 31. Stop B4. One of the Tepexitl tuff-ring features are the bomb sags produced by ballistic clasts emplaced in the direction to the viewer.

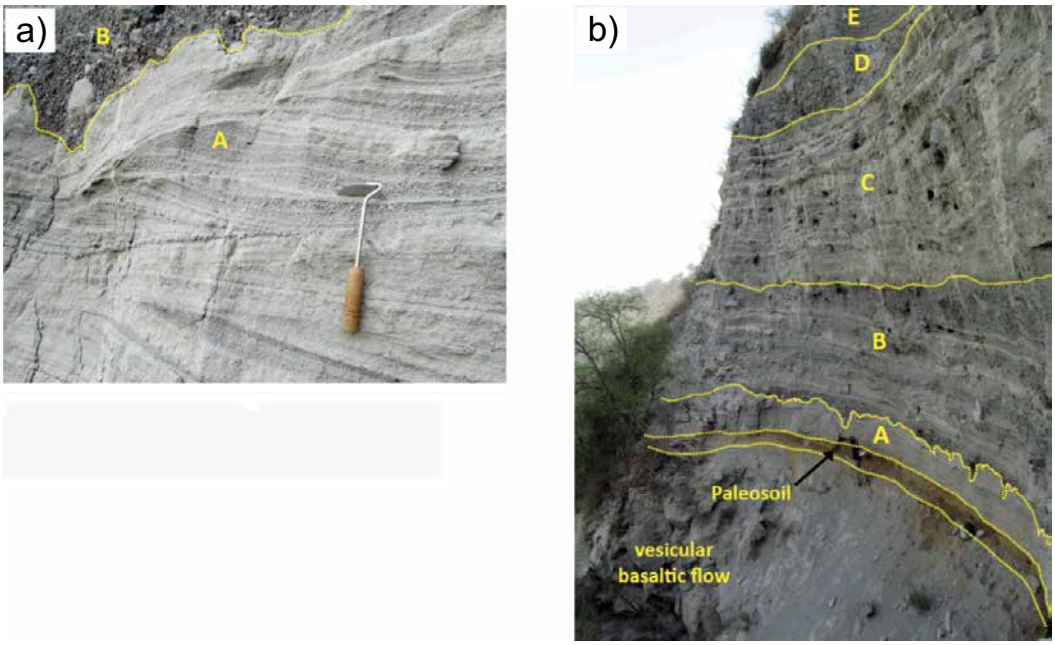

Figure 32. Stop C1.1 Photographs of Aljojuca maar: A) Lowermost unit showing a characteristic cross-bedded sequence overlaid by an unconformable coarse breccia horizon; B) Western section showing eruptive units "a", "b" and "c" the lower maar-forming sequence shown in figure 20, overlying a bown soil and the country rock composed by a basaltic lava flow, exposed to the left.

Stop C2.2. cinder cones inside the crater
Location: UTM 14 Q 653776/ 2115399

The second stop is at Tecuitlapa inner crater and will focus on the scoria cones and spatter that formed after the maar-forming eruptions were finished (Figure 33b). These cones appear to mark the location of the dike that fed the entire eruption, with migration to the west during the "wet" portion of the eruption followed by eastward vent migration during the drying-out phase.

§

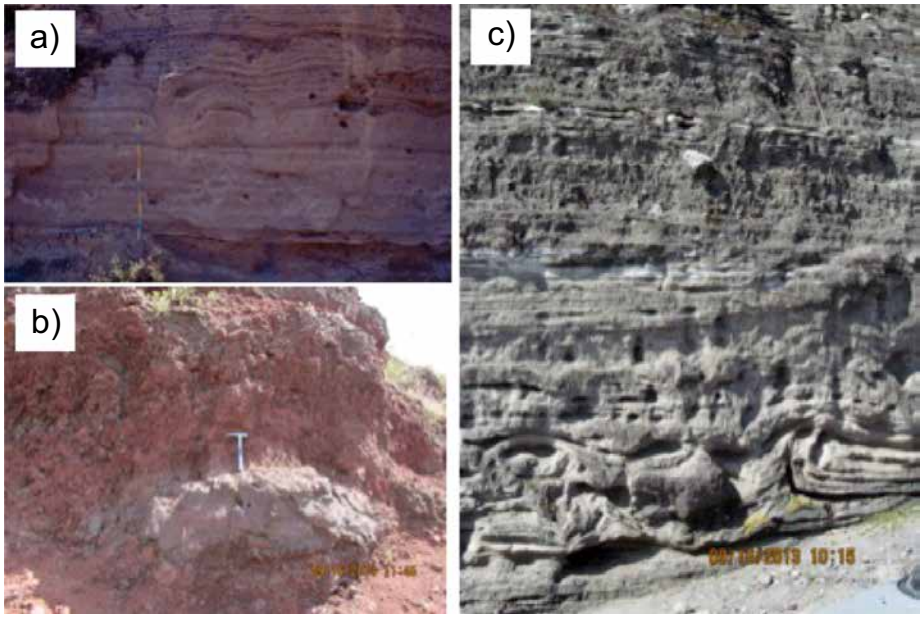

Figure 33. Stop C2. Photographs of the Tecuitlapa crater: a) Surge-dominated stratified unit at the base of the eruptive sequence, showing some bomb sags (Stop C2.1); b) Spatter breccia with very large bombs at the youngest scoria cone in the eastern part of the crater interior (Stop C2.1); c) Spectacular deformation produced by a large ballistic bomb at the middle part of the sequence, causing inverted stratigraphy of a few layers (Stop C2.2)

REFERENCES

Abrams, M., Siebe, C., 1994. Cerro Xalapaxco: an unusual tuff cone with multiple explosion craters, in central Mexico (Puebla). Journal of Volcanology and Geothermal Research, v. 63, 183-199.

Alcocer, J., Escobar, E., Lugo, A., Peralta L., 1998. Littoral benthos of the saline crater lakes of the basin of Oriental, Mexico. International Journal of Salt lake Reasearch 7, 97-108.

Austin-Erickson, A., 2007. Phreatomagmatic eruptions of rhyolitic magma: A case study of Tepexitl tuff ring, Serdan-Oriental Basin, Mexico: Flagstaff, Arizona, USA, Northern Arizona University, M.S. thesis, 194 pp.

Austin-Erickson, A., Ort, M., Carrasco-Núñez, G., 2011. Rhyolitic phreatomagmatism explored: Tepexitl tuff ring (Eastern Mexican Volcanic Belt): Journal of Volcanology and Geothermal Research, 201, 325-341. doi:10.1016/j.volgeores.2010.09.007.

Carrasco-Núñez, G., 2000. Structure and proximal stratigraphy of Citlaltépetl Volcano (Pico de Orizaba), Mexico, *in* Delgado-Granados, H., Aguirre-Díaz, G., Stock, J. (Eds.), Cenozoic Volcanism and Tectonics ofMexico: Geological Society of America Special Paper, vol. 334, 247-262.

Carrasco-Núñez, G., and Branney, M.J., 2005, Progressive assembly of a massive layer of ignimbrite with normal-to-reverse compositional zoning: the Zaragoza ignimbrite of central Mexico: Bulletin of Volcanology, v. 68, p. 3-20.

Carrasco-Núñez, G. and Riggs, N., 2008. Polygenetic nature of a rhyolitic dome and implications for hazard assessment: Cerro Pizarro volcano, Mexico. Journal of Volcanology and Geothermal Research, 171, 307-315.

Carrasco-Núñez, G., Ort, M., Romero, C., 2007. Evolution and hydrological conditions of a maar volcano (Atexcac crater, Eastern Mexico), *in* Martin, U., Németh, K., Lorenz, V., White, J. (eds.) Maar-diatreme volcanism and associated processes: Journal of Volcanology and Geothermal Research, 159, 179-197.

Carrasco-Núñez, G., Gómez-Tuena, A., Lozano, L., 1997. Geologic map of Cerro Grande volcano and surrounding area, Central Mexico: Geological Society of America Map and Chart Series MCH 081, 10 pp.

Carrasco-Núñez, G., Díaz-Castellón, R., Siebert, L., Hubbard, B., Sheridan, M. F., Rodríguez, S. R., 2006. Multiple edifice-collapse events in the Eastern Mexican Volcanic Belt: the role of sloping substrate and implications for hazard assessment, *in* Tibaldi, A. and Lagmay, A., (eds.) The effects of basement structural and stratigraphic heritages on volcano behaviour: Journal of Volcanology and Geothermal Research, 158, 151-176.

Carrasco-Núñez, G., Siebert, L, Díaz-Castellón, R., Vázquez-Selem, L., Capra, L., 2010. Evolution and hazards of a long-quiescent compound shield-like volcano: Cofre de Perote, Eastern Trans-Mexican Volcanic Belt: Journal of Volcanology and Geothermal Research, 197, 209-224.

Carrasco-Núñez, G., McCurry, M., Branney, M.J., Norry, M.,Willcox, C., 2012. Complex magma mixing, mingling, and withdrawal associated with an intraplinian ignimbrite eruption at a large silicic caldera volcano: Los Humeros of central Mexico: Geological Society of America Bulletin 124, 1793-1809.

Dávila-Harris, P., Carrasco-Núñez, G., 2014. An unusual syn-eruptive bimodal eruption: The Holocene Cuicuiltic Member at Los Humeros caldera, Mexico: Journal of Volcanology and Geothermal Research, 271, 24-42.

De León, L., Carrasco-Núñez, G., 2014. Stratigraphy of the Aljojuca maar (Puebla, Mexico) in 5th International Maar Conference: Querétaro, Qro., México, November 2014, Centro de Geociencias, Universidad Nacional Autónoma de México, Abstracts Volume.

Ferriz, H., Mahood, G., 1984. Eruption rates and compositional trends at Los Humeros volcanic center, Puebla, Mexico: Journal of Geophysical Research, v. 89(B10), 8511-8524.

Gasca-Durán, A., 1981. Génesis de los lagos-cráter de la cuenca de Oriental: Colección Científica Prehistórica , 98, 57 pp.

Gómez-Tuena, A., Carrasco-Núñez, G., 2000. Cerro Grande volcano: the evolution of a Miocene stratocone in the early trans-Mexican Volcanic Belt: Tectonophysics 318, 249-280.

Houghton, B.F., C.J.N. Wilson, P. Del Carlo, M. Coltelli, J.E. Sable, R. Carey, 2004, The influence of conduit processes on changes in style of basaltic Plinian eruptions: Tarawera 1886 and Etna 122 BC: Journal of Volcanology and Geothermal Research, 137, 1-14.

Kazmierczak, J., Kempe, S., Kremer, B., López-García, P., Moreira, D., Tavera, R., 2011. Hydrochemistry and microbialites of the alkaline crater lake Alchichica, Mexico: Facies 57, 543-570.

Keating, G.N., Valentine, G.A., Krier, D.J., Perry, F.V. 2008, Shallow plumbing systems for small-volume basaltic volcanoes: Bulletin of Volcanology 70, 563-582.

Negendank, J., Emmermann, R., Krawczyk, R., Mooer, F., Tobschall, H.,Werle, D., 1985. Geological and geochemical investigations on the eastern TMV: Geofísica Intnational 24, 477-575.

Ordóñez, E., 1905. Los xalapaxcos del estado de Puebla: Instituto de Geología. México 350-393.

Ordóñez, E., 1906. Los xalapaxcos del estado de Puebla, 2a parte: Instituto de Geología, México 350-393.

Ort, M., Carrasco-Núñez, G., 2009. Lateral Vent Migration during Phreatomagmatic and Magmatic Eruptions at Tecuitlapa Maar, East-Central Mexico; Journal of Volcanology and Geothermal Research, 181, 67-77.

Riggs, N., Carrasco-Núñez, G., 2004. Evolution of a complex, isolated dome system, Cerro Pizarro, central Mexico: Bulletin of Volcanology 66, 322-335.

Rodríguez-Elizarrarás, S.R., 2005. Geology of the Las Cumbres Volcanic Complex, Puebla and Veracruz states, Mexico: Revista Mexicana de Ciencias Geológicas, 22, 181-198.

Romero, C., 2000. Estratigrafía del cráter Atexcac. Facultad de Ingeniería, Universidad Nacional Autónoma de México, Bch. Thesis, 98 pp.

Siebe, C., Macías, J.L., Abrams, M., Rodríguez, S., Castro, R., Delgado, H., 1995. Quaternary explosive volcanism and pyroclastic deposits in east central Mexico: implications for future hazards: Geological Society of America Field Guide, 1-47.

Siebe, C., Macías, J.L., Abrams, M., Rodríguez, S., Castro, R., Delgado, H., 1995. Quaternary explosive volcanism and pyroclastic deposits in East central Mexico: implications for future hazards: Geological Society of America Field Guide 1-47.

Siebert, L., Carrasco-Núñez, G., 2002. Late-Pleistocene to precolumbian behind-the-arc mafic volcanism in the eastern Mexican Volcanic Belt; implications for future hazards: Journal of Volcanology and Geothermal Research, 115, 179-205.

Suter , M., López, M., Quintero, L., Carrillo, M., 2001. Quaternary intra-arc extension in the central Trans-Mexican volcanic Belt: Geogical Society of America Bulletin 113, 693-703.

Viniegra, F., 1965, Geología del Macizo de Teziutlán y la Cuenca Cenozoica de Veracruz: Boletín Asociación Mexicana Geólogos Petroleros, v. 17, p. 101-163.

White, J.D.L., Schmincke, H.L., 1999. Phreato-magmatic eruptive and depositional processes during the 1949 eruption on La Palma Canary Islands: Journal of Volcanology and Geothermal Research, 94, 283-304

Willcox, C.P., 2011. Eruptive, magmatic and structural evolution of a large explosive caldera volcano: Los Humeros, Central Mexico: Leicester, U.K. University of Leicester, PhD Thesis.

Yáñez, C., and García, S., 1982. Exploración de la región geotérmica Los Humeros – Las Derrumbadas, estados Puebla y Veracruz: Comisión Federal de Electricidad (México), 29, 98.

Zimmer, B.W., 2007. Eruptive variations during the emplacement of Cerro Pinto dome complex, Puebla, Mexico; Northern Arizona University, MS thesis, 119 pp.

Zimmer, B., Riggs, N.R., Carrasco-Núñez, G. 2010. Evolution of tuff ring-dome complex: the case study of Cerro Pinto, eastern Trans-Mexican Volcanic Belt: Bulletin of Volcanology, 72, 1233-1240.

§

We acknowledge our sponsors for their support to this meeting:

UNIVERSIDAD NACIONAL
AUTÓNOMA DE MÉXICO

Centro de Geociencias
Universidad Nacional Autónoma de México
Querétaro, Mexico, September 2014

http://maar2014.geociencias.unam.mx